

## CHAPTER 14

# Nuclear Plant Materials and Corrosion

prepared by

Dr. Derek H. Lister and Dr. William G. Cook

University of New Brunswick

### Summary:

*The choice of materials of construction of a nuclear reactor, while important in terms of plant capital cost, is crucial to the safe and economic operation of the unit throughout its design lifetime; it also affects decisions about plant life extension. Most of the failures of nuclear systems involve the degradation of materials as they interact with their environments, indicating that chemistry control within systems should be formulated as materials are selected. All of the three major process systems of a CANDU reactor – the primary coolant, the moderator and the secondary coolant – have a variety of materials of construction, so the control of system chemistry in each is a compromise based on the characteristics of the interactions between the system materials and the environment, including the effects of irradiation on both the material and the coolant or moderator. Ancillary systems, such as those providing condenser cooling water or recirculating cooling water, have similar constraints on material choice and chemistry control. Components such as concrete structures, cabling and insulation, although not necessarily associated with process systems, may also be critical to safety or plant operation and must have their materials chosen with care. This chapter describes the materials of construction of the main systems and components of a CANDU reactor and shows how they interact with their environments.*

### Table of Contents

1	Introduction .....	3
2	Materials for Nuclear Applications .....	4
2.1	Metallurgy and Irradiation Effects.....	4
2.2	Materials of Construction.....	7
3	CANDU Process Systems and their Materials .....	21
3.1	Major Process Systems.....	21
3.2	Ancillary Process Systems.....	23
3.3	Supporting Structures and Components.....	25
4	Corrosion and Material Degradation in Nuclear Reactor Systems .....	27
4.1	General Corrosion.....	27
4.2	Flow-Accelerated Corrosion (FAC).....	35
4.3	Galvanic Corrosion.....	39
4.4	Stress-Corrosion Cracking & IGA .....	42
4.5	Crevice Corrosion & Pitting .....	45
4.6	Fretting Wear & Flow-Induced Vibration .....	48
4.7	Hydrogen Effects .....	49

4.8	Microbiologically-Induced Corrosion (MIC).....	49
5	References.....	51
6	Acknowledgements.....	54

## List of Figures

Figure 1.	Unit cell configurations of some common metallic crystal structures (after Callister) ...	5
Figure 2.	Grain structure for low-alloy (UNS G10800), austenitic (316 SS) steels and Zircaloy 4 (ASM, 2004). .....	5
Figure 3.	Effect of neutron irradiation on the stress/strain properties of materials with cubic crystal structures (after Was, 2006).....	6
Figure 4.	Partial iron-carbon phase diagram (after Callister).....	10
Figure 5.	Schematic Cross-Section through Magnetite Film on Carbon Steel [Lister, 2003] .....	31
Figure 6.	Scanning Electron Micrograph of Magnetite Film formed on Carbon Steel during an 1100-h Exposure in High-Temperature Water [Lister, 2003] .....	31
Figure 7.	Schematic diagram of Zircaloy corrosion in high-temperature water, showing three regions (dotted line indicates early assumed pre-transition cubic and post-transition linear kinetics) [Hillner et al, 2000].....	33
Figure 8.	Scalloped surface of outlet feeder from Point Lepreau CANDU .....	36
Figure 9.	(a) Effect of temperature and flow on FAC at pH <sub>25°C</sub> 9.0 with ammonia; (b) Effect of temperature and pH on the solubility of magnetite. ....	38
Figure 10.	The overall mechanism of flow-accelerated corrosion.....	38
Figure 11.	Examples of transgranular (TGSCC) (a) and intergranular (IGSCC) (b) stress corrosion cracking in stainless steel and brass respectively (after Fontana 1986).....	42
Figure 12.	Typical sensitization mode and IGA of Type 304 stainless steel (after Fontana 1986)	44
Figure 13.	Initial (A) and final (B) stages in the development of crevice corrosion of a metal M (Fontana, 1986).....	46
Figure 14.	Self-perpetuating corrosion pit (after Fontana, 1986).....	47
Figure 15.	An undercut pit and surface wastage from overlapping pits.....	47

## List of Tables

Table 1.	Compositions of commonly used zirconium alloys in CANDUs.....	8
Table 2.	Standard compositions of commonly used ferritic, martensitic and austenitic steels in CANDUs.....	14
Table 3.	Compositions of commonly used nickel alloys in nuclear power plants.....	15
Table 4.	Severity of radiation-induced damage of common polymers.....	20
Table 5.	The galvanic series for important metals .....	41
Table 6.	Biocides used in industrial water systems.....	51

# 1 Introduction

The performance of power-producing systems has always been limited by the properties of engineering materials and their interactions with the environment. Since the early days of industrial steam generation in the seventeenth and eighteenth centuries, for example, the ever-increasing need for power for new factories created a steady demand for larger boilers and increasingly severe steam conditions. Materials selection was based on limited knowledge of corrosion, especially stress corrosion cracking as the consequence of chloride and oxygen contamination of the water used in the boilers and catastrophic failures of equipment occurred frequently.

As late as the end of the nineteenth century, hundreds of steam plant explosions accompanied by large numbers of casualties were being recorded every year in Europe and North America. The causes were generally linked to the failure of riveted joints or poorly worked steel plate in fire-tube boilers. The innovation of the water-tube boiler and the understanding of localized corrosion of steels in high-temperature water were major factors that led to much safer equipment - even as operating conditions continued to become more severe. The major consequence of these failures was the development of codes and standards for pressure retaining components, the ASME Pressure Vessel Code in North America for example, which dictate the acceptable design and construction practices for materials produced to particular specifications.

Today, the risk of catastrophic failure of a power-producing system is low. This can be attributed to the strict adherence to the standards that are imposed on component designers and manufacturers as well as on plant operators. The setting of these standards clearly involves a thorough knowledge of the properties of the materials of construction and an understanding of their behaviour in the local environment. That environment may itself be adjusted for overall optimum performance by specifying optimum chemistry control strategies. The prime example of such chemistry control is the specification of an alkalinity level in the feedwater systems of steam-raising plants, including nuclear secondary coolants, which is necessary to minimize corrosion of piping and components and to keep systems clean of dissolved and particulate corrosion products and impurities. In a nuclear reactor core, materials must be able to withstand not only the operational conditions (pressure, temperature and water chemistry) but must show minimal degradation from the effects of radiation (high gamma and neutron flux). Radiation effects on materials may include loss of ductility, shape change from radiation enhanced creep and growth and enhanced corrosion resulting from hydrogen ingress (deuterium ingress for the case of heavy water systems).

While the current performance record of power plants is generally good, technology is not standing still. The push for bigger returns on capital investment and the accompanying trends towards higher plant efficiencies and longer component lifetimes lead to even more severe operating conditions in power systems. Inevitably, the demands on the materials of construction escalate. The predominant materials of construction in steam-raising equipment and nuclear systems are the metals and alloys. Their interaction with the operating environment very much dictates the chemistry control to be practised by plant operators.

## 2 Materials for Nuclear Applications

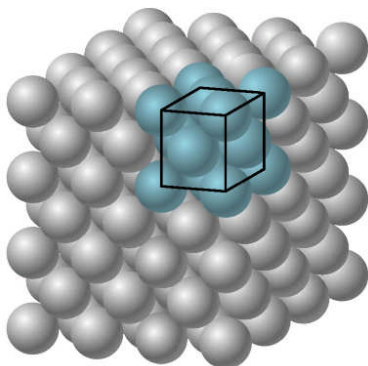
As described above, materials of construction for nuclear applications must be strong, ductile and capable of withstanding the harsh environment to which they are subjected. Furthermore, for materials used in the core of a nuclear reactor, it is important that they have specific properties such as low neutron absorption and high resistance to radiation-induced creep, hardening and the associated loss of ductility so that reactors can operate for the decades expected by plant owners. Thus, nuclear materials must be selected or specified based upon their strength and interactions with the environment (including the effects of radiation), all of which are dependent upon the metallurgy of the material.

### 2.1 Metallurgy and Irradiation Effects

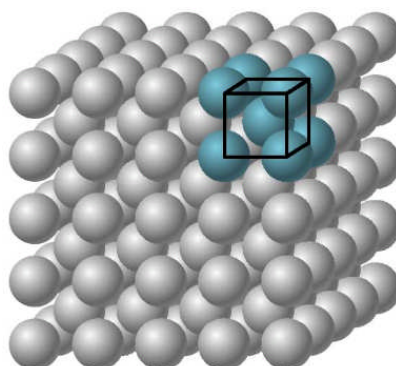
#### 2.1.1 Crystal Structure and Grain Boundaries

**All metals used in power plant construction are crystalline in nature, meaning that they have a defined and consistent crystal structure. Three of the basic and most observed crystal structures are shown in**

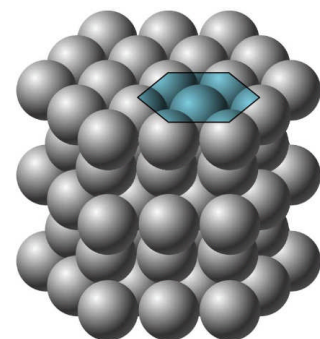
Figure 1, namely: face-centred cubic (FCC), body-centred cubic (BCC) and hexagonal close-packed (HCP). Upon cooling from a melt during the production of a metal or alloy, individual crystals nucleate and coalesce as the material solidifies. As the individual crystals grow together they eventually meet and combine as an assemblage of crystal grains, which will likely not have the same orientation of the crystal lattice. This leads to the development of grain boundaries in the material, where the atoms along the boundary between the two grains have elongated metallic bonds leading to slightly elevated boundary energies than those within the bulk of the individual crystal. The grain boundaries are thus slightly more active than the individual grains and can act as diffusion short-circuits or locations for the development of precipitates such as carbides. The materials used in nuclear power plants are thus termed polycrystalline due to the grain/grain-boundary structure.



(a) FCC structure



(b) BCC structure



(c) HCP structure

**Figure 1. Unit cell configurations of some common metallic crystal structures (after Callister)**

The grains of a metal or alloy may be engineered through appropriate heat treatments (hot and cold working and annealing for example) to be of a specific size and/or orientation to meet a specified purpose. Small-grained metals (1 – 25  $\mu\text{m}$ ) will have more grain boundaries and may be more affected by phenomena such as high-temperature creep or radiation-induced creep. Examples of the metallurgy and microstructure of ferritic steel, austenitic stainless steel and zirconium are shown in Figure 2. Note that the grain structure, size and orientation may play significant roles in the specific materials properties such as strength, conductivity and creep resistance.

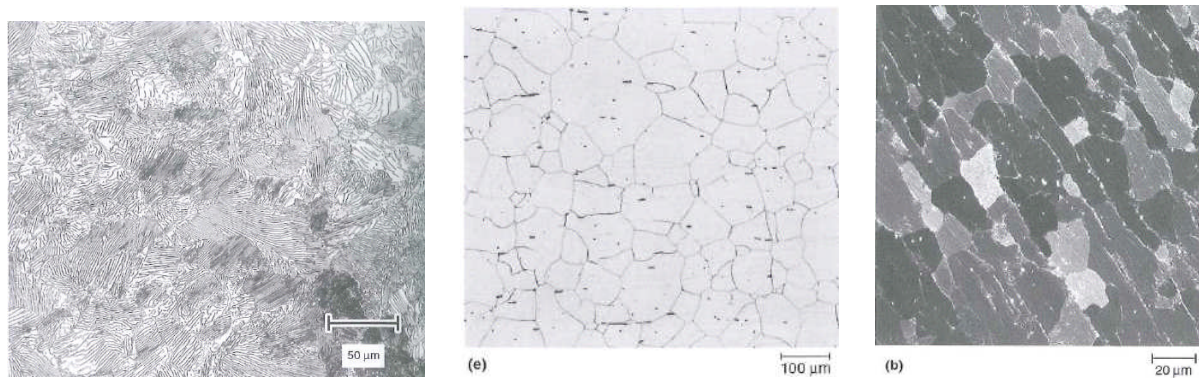


**Figure 2. Grain structure for low-alloy (UNS G10800), austenitic (316 SS) steels and Zircaloy 4 (ASM, 2004).**

**2.1.2 Irradiation effects on materials**

The effects of irradiation on materials may be manifest in several ways, the most dramatic being the dislodging or dislocation of a random atom in the crystal lattice to a new location. During neutron bombardment, the energy dissipated by the neutron upon collision with a metal atom can create new defects in the crystal structure, typically “interstitial” sites where the dislocated atoms come to rest between the regular bonding sites in the crystal structure and “vacancy” sites left where the atoms were originally stationed. The pair (interstitial/vacancy) is termed a Frenkel pair and is a key phenomenon associated with radiation damage in polycrystalline materials. The damage induced in the material is additive and substantial, considering that in a CANDU reactor the overall neutron flux may be  $2 \times 10^{17}$  neutrons/ $\text{m}^2\text{s}$  and the flux in enriched reactors (light water reactors, breeders etc.) may be several times higher. Radiation damage is typically measured in “displacements per atom” (dpa) and the dose can be as high as 10 – 30 dpa after 30 years of operation.

The fact that neutron bombardment creates interstitials and vacancies within the material gives rise to changes in the physical dimensions and the mechanical properties of the material when placed under stress. The creation of vacancies within the material leads to swelling, elongation and growth whereas production of interstitials can cause the material to shrink. The energy

dissipated by radiation may induce phase changes within the material or promote segregation of alloying constituents, both phenomena will affect the material's strength and ductility. Overall, the mechanical properties and dimensions of a material under irradiation will change and the effect ultimately leads to challenges for the integrity of the components that make up a nuclear reactor. Each mechanical effect is described briefly below, more details can be found in *Fundamental of Radiation Materials Science* (Was, 2007).

### Irradiation Hardening

When a polycrystalline material is placed under stress it will stretch elastically with increasing stress/strain up to the yield point of the material. Additional strain beyond the yield strength leads to plastic deformation whereby the original shape and dimensions of the material can no longer be attained with the relaxation of the strain. Plastic deformation, at the atomic level, is induced when the atoms in the crystal lattice slip, which typically occurs on slip planes in the matrix. When a material is irradiated by particles (neutrons) producing Frenkel pairs, the effect of the interstitial/vacancy sites is to provide barriers to the normal slip planes within the material. This effectively increases the yield strength, which will increase continuously in proportion to the increasing radiation dose (dpa). Figure 3 shows the effect of neutron irradiation on the yield stress/strain for materials with the FCC and BCC crystal structures [Was, 2006].

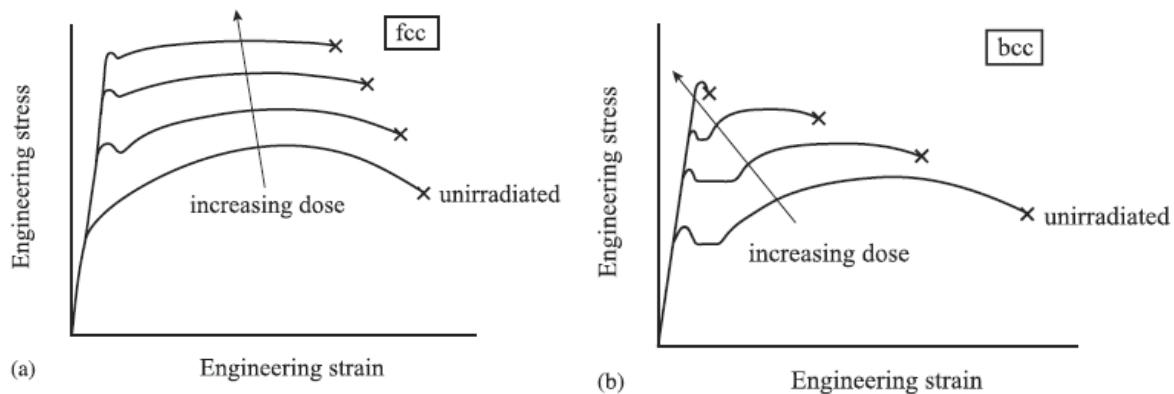


**Figure 3. Effect of neutron irradiation on the stress/strain properties of materials with cubic crystal structures (after Was, 2006).**

### Irradiation Creep and Growth

All metals will exhibit creep over time when exposed at high temperatures and under operational stress. Thermal creep is a diffusion-based migration of atoms and vacancy sites within the metal's lattice, which typically requires a minimum operating temperature before its effects are observed – generally the operating temperature must be greater than  $0.3T_m$ , where  $T_m$  is the melting temperature of the metal. Since diffusion is the primary mechanism at play for thermal creep it typically increases exponentially with increasing temperature following an Arrhenius law. As described above, particle bombardment or irradiation of a metal creates interstitials and vacancies within the metal's lattice, effectively mimicking the effects of thermal creep of the metal only occurring at much lower temperatures than those required for significant thermal

creep alone. Since the diffusion rates of vacancies and interstitials are unaffected by irradiation (diffusion is a temperature dependent phenomenon), irradiation creep is more complex in its mechanism and involves the preferential absorption of interstitials under the action of strain in the material and phenomena such as the “climb and glide” of the dislocations over barriers to the diffusion process. Irradiation creep is preferential in directions perpendicular to the applied stress i.e. pipes will tend to elongate due to irradiation creep.

For materials that do not have a cubic crystal structure (zirconium being the most relevant with an HCP structure below 862°C), grain distribution and orientation (described as the material’s texture) play significant roles in irradiation creep and growth. The distinction made between creep and growth is that the former is the elongation of a material under applied stress while the latter occurs even when no external stress is applied. The material’s texture gives rise to anisotropy in the preferred crystallographic planes by which the material will stretch under an induced strain as well as grow in a preferred direction during creep. Thus, the creep characteristics of non-cubic crystal materials (zirconium and zirconium alloys) are highly dependent upon the applied stress as well as the operational temperature.

### Irradiation Embrittlement

As a metal gains strength upon particle irradiation, it will also tend to lose its ductility, becoming hard and brittle with increasing damage and radiation dose. The material’s yield strength increases through build-up of dislocations along barriers to atom migration, but other effects such as the precipitation of secondary and tertiary phases within the material can change the mechanical properties dramatically. Materials that are typically ductile and not susceptible to brittle fracture in an un-irradiated environment may cleave and fracture excessively upon irradiation due to the increasing hardness and loss of ductility.

## **2.2 Materials of Construction**

### **2.2.1 Zirconium**

Zirconium is the eleventh most abundant element in the earth’s crust making it more prevalent than the common transition metals copper, lead, nickel and zinc. It occurs naturally as the minerals zircon (zirconium silicate –  $ZrSiO_4$ ) and zirconia (zirconium oxide –  $ZrO_2$ ) and always in conjunction with 0.5 – 2.5% hafnium (Hf), a metal that has very similar chemical and physical properties making it difficult to separate the two elements. Zirconium or, more specifically, the alloys fabricated from it are the most important of the nuclear reactor materials. They are resistant to corrosion in many process environments, nuclear heat transport systems in particular, and they have excellent nuclear properties making them the predominant materials for construction of in-core components (fuel sheathing, pressure tubes and calandria tubes). Zirconium itself has a neutron absorption cross-section of 0.18 barns, making it nearly transparent to the thermal neutrons in a water-cooled and -moderated reactor. Zirconium alloys used in nuclear reactors must be highly processed to keep the hafnium concentration below 100 ppm since its neutron absorption cross-section is 102 barns, nearly 600 times that of zirconium. Higher concentrations of hafnium would increase the parasitic absorption of neutrons in the

reactor core and reduce the fuel burn-up. Pure zirconium has an HCP structure that transforms to BCC at 862°C before melting at 1850°C. It is a reactive metal that combines easily with oxygen, hydrogen, nitrogen, carbon and silicon and in air retains its metallic lustre because of a very thin but protective zirconia ( $ZrO_2$ ) oxide layer. A protective but thicker zirconia layer is retained during exposure to high-temperature water, making zirconium alloys ideal for service in water-reactor cores. The pure metal is alloyed with small amounts of elements such as tin, chromium, iron, nickel and niobium to improve mechanical strength, corrosion resistance and to reduce hydrogen pickup. In CANDUs, the alloy Zircaloy-2 is used for the calandria tubes and was the initial choice as the pressure tube material. Zircaloy-2 contains 1.2 – 1.7 weight percent Sn, 0.07 – 0.2 weight percent Fe, 0.05 – 0.15 weight percent Cr and 0.03 – 0.08 weight percent Ni. It is also the material used for BWR fuel cladding. For fuel sheathing in CANDUs and fuel cladding in PWRs, Zircaloy-4 was developed and used because it was observed to have a lower overall corrosion rate and a reduced tendency to pick up hydrogen. It has a similar composition to that of Zircaloy-2 except for the nickel content, which is reduced to a maximum of 0.007 weight percent, and the iron content, which is increased to 0.18 – 0.24 weight percent. The compositions of zirconium alloys used in CANDU reactors are shown in Table 1. Comparatively recent developments in fuel cladding technology for PWRs are the Westinghouse alloy ZIRLO, which contains 0.7 – 1.0 weight percent Sn and 1.0 weight percent Nb, and the Areva variant M5, which has no Sn and 0.8 – 1.2 weight percent Nb. A Zr-1%Nb alloy was developed and used for decades as the fuel cladding material in the Russian VVERs and the Westinghouse and Areva alloys are modifications from the original Russian composition. They are reputedly more corrosion-resistant and have lower hydrogen pick up than Zircaloy-4 under high fuel burn-up. Similarly, for BWR cladding, Westinghouse has developed the alloy ZrSn, which is Zr with 0.25 weight percent Sn. The pressure tubes in CANDUs are made of Zr-2.5%Nb, an alloy of Zr and Nb with the latter within the range 2.4 – 2.8 weight percent. This too is a modification of Russian alloys developed for the RBMK reactors.

**Table 1. Compositions of commonly used zirconium alloys in CANDUs.**

Common designation	UNS #	chemical composition (wt%)						
		Sn	Nb	Fe	Cr	Ni	O (ppm)	Hf (ppm)
Zr 702	R60702			Fe + Cr < 0.2			< 0.16%	4.5%
Zircaloy 2	R60802	1.2-1.7		0.07-0.2	0.05-0.15	0.03-0.08	1200-1400	100
Zircaloy 4	R60804	1.2-1.7		0.18-0.24	0.07-0.13	0.03-0.08	1200-1400	100
Zr-2.5%Nb	R60901		2.4-2.8				1200-1400	100

## 2.2.2 Steels

### Carbon Steels

The most widely used materials in power-producing systems are the steels, which are basically alloys of iron and carbon but which may also contain other metals as minor or major alloying elements. The alloying elements impart desired properties such as strength, hardness or corrosion resistance to the steel.

Pure iron at ambient temperatures has a body-centred cubic (BCC) crystal structure, in which the atoms making up the unit cell of the crystal lattice are conveniently pictured as occupying the corners of a cube with an atom at the cube centre. Figure 1 shows illustrations of unit cell configurations of typical metals. The BCC phase is called  $\alpha$ -iron or ferrite, which in pure iron is stable below 912°C. Above this temperature the  $\gamma$ -iron or austenite phase with a face-centred cubic (FCC) crystal structure is stable up to 1394°C. The FCC unit cell has an atom at each corner of a cube and one at the centre of each face as shown in Figure 1. Above 1394°C another BCC phase,  $\delta$ -iron, is stable up to the melting point at 1538°C. The relatively small atoms of carbon that can exist in solid solution in these structures are in random interstitial positions between the iron atoms. The carbon concentration determines the stability limits of the phases.

As the portion of the iron-carbon phase diagram that is pertinent to steels indicates, carbon has a low solubility in ferrite. Figure 4 illustrates the iron-carbon phase diagram, in which the regions of stability of the different steel phases are shown in terms of their composition and temperature. The maximum in ferrite is 0.02 weight percent and occurs at a temperature of 727°C. At temperatures much above and below this, the solubility declines to almost zero. The common carbon steels, however, have carbon contents ranging up to about 2.0 weight percent, and they are quite stable at temperatures below 727°C. To accommodate the carbon, these steels are composed of more phases than just the ferrite. As the phase diagram indicates, for carbon contents up to 6.7 weight percent, which is the amount of carbon in the compound  $\text{Fe}_3\text{C}$  (iron carbide or cementite), two distinct phases exist together in equilibrium - ferrite and cementite. The proportions depend upon the overall amount of carbon in the mixture but are not affected much by temperature below the 727°C region.

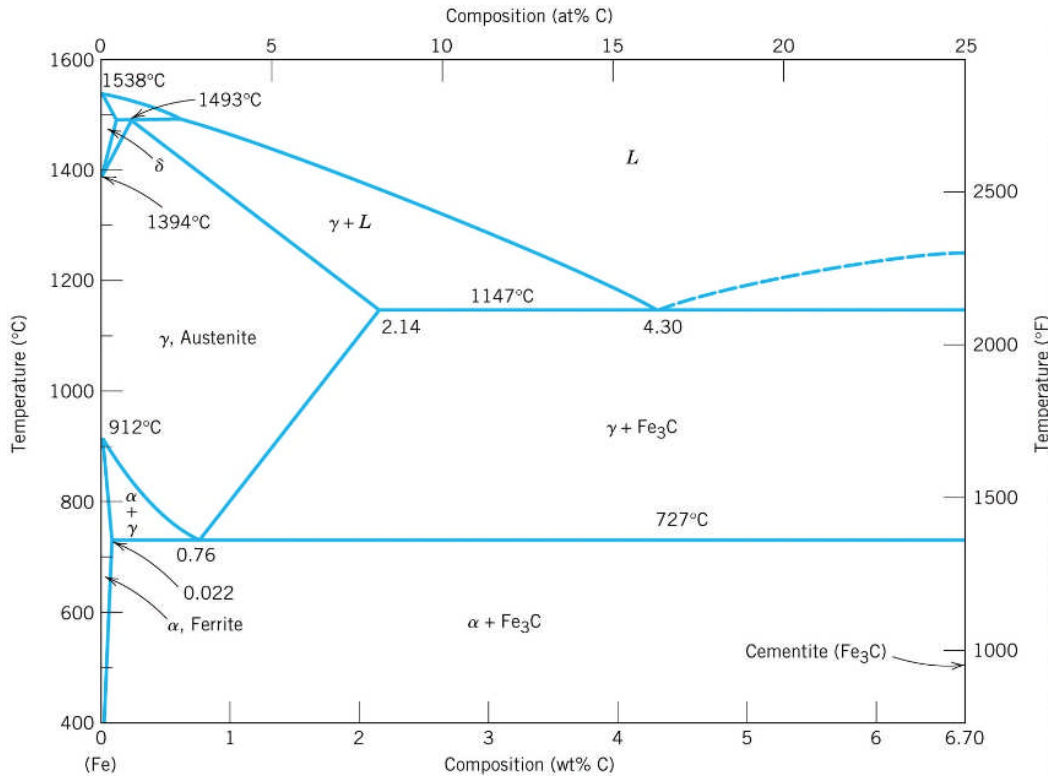


**Figure 4. Partial iron-carbon phase diagram (after Callister)**

In the aggregate of metal grains and intercalating grain boundaries that make up a carbon steel, some grains may be ferrite or cementite and some will be a two-phase ferrite-cementite composite. The composite grains are formed from alternating microscopic layers or lamellae of ferrite and cementite in a structure called pearlite. The size of the grains, the proportions of the different phases, and the details of the pearlite structure govern the mechanical properties of the steel. In general, higher carbon contents produce steels that can be made stronger and harder by heat treatment and mechanical working to control grain structure and properties. At carbon contents above the 2 weight percent value, however, the material enters the range of the cast irons and starts to become brittle and lose properties such as ductility and toughness that are important for many power plant applications. For most boiler applications and piping in general, steels with carbon contents of 0.20 weight percent or less are employed. Equipment such as pumps, valves, turbine components etc. requiring stronger or harder material commonly use steels with carbon contents up to 0.50 weight percent or more.

The phase diagram in Figure 4 indicates that the high-temperature  $\gamma$ -phase of iron, austenite, can contain a relatively large amount of carbon in solid solution - up to 2.1 weight percent at 1148°C. This is because the FCC structure of austenite, although having a higher atomic packing fraction than the BCC structure of ferrite (0.74 versus 0.68), has more interstitial sites to accommodate the small carbon atoms (by contrast, the more open structure of BCC leads to higher rates of solid-state diffusion). Note that austenite is stable down to the eutectoid temperature 727°C, below which it transforms into the lamellar pearlite. A heat treatment may then consist of heating a carbon steel to a temperature that puts it in the austenite region, where the carbon is completely miscible. Cooling at a controlled rate to below 727°C will then

promote the transformation to pearlite, pearlite-ferrite or pearlite-cementite, depending upon whether the total amount of carbon is respectively equal to, less than or greater than the eutectoid composition of 0.77 weight percent.

If, during the heat treatment, the austenitized steel at high temperature is cooled suddenly or quenched (by plunging into cold water, oil, etc.) rather than cooled in a slow controlled fashion, a different phase called martensite is produced. This has a body-centred tetragonal (BCT) crystal lattice, the unit cell of which can be viewed as a BCC structure stretched in the direction of one of the cube axes as shown in Figure 1. Carbon atoms can then be accommodated in interstitial positions between iron atoms in the direction of elongation or in the centres of the basal planes and can thereby stay in solid solution. Martensite is a very hard, strong but quite brittle material that has a metastable structure (and therefore does not appear on the phase diagram, which shows equilibrium states only). It nonetheless survives indefinitely at ambient temperature.

The formation of martensite can impart very useful properties to steel. Thus, by selective austenitizing, quenching and then tempering for a given period at temperatures near the eutectoid point (727°C), the amount of martensite in a steel can be controlled and a hard, strong material that is not too brittle can be obtained. Other iron-carbon phases called bainite and spheroidite are also formed during selective heat treatments to produce steels with specific characteristics of strength, ductility and toughness.

### Alloying elements

Metals other than iron may be added to steel to impart desired mechanical properties or corrosion resistance - particularly useful for service at high temperature. The atoms of alloying metals are generally in substitutional solid solution, meaning that they take the place of iron atoms in the crystal lattice. If the metal addition is less than 5 weight percent what is commonly called a low-alloy steel results, while additions greater than 5 percent produce the intermediate- and high-alloy steels. Note, however, that the plain carbon steels often contain small amounts of elements such as manganese, phosphorus or sulphur - generally less than 1 weight percent - as residuals from the steelmaking process or they may be added for specific reasons such as improved machinability. Manganese in particular can impart desirable mechanical properties to steel and in fact may be added deliberately to form low-alloy manganese steel with a marked resistance to wear. Table 2 shows the typical compositions of various steels and stainless steels commonly used in CANDUs.

Plain carbon steel and manganese steel are used extensively for general construction steelwork in power systems and in non-nuclear boiler construction for tubing and components that experience temperatures below about 500°C. They are also employed in the secondary or steam-raising systems of nuclear power plants and constitute a major proportion of the piping in the primary coolant systems of heavy water reactors such as the CANDU reactor, which operate below about 320°C, and for steam generator tubes and piping in carbon-dioxide-cooled Magnox reactors, which operate below about 360°C. As the service temperature increases the amount of alloying is necessarily increased to impart resistance to creep and scaling. For example, boiler superheater tubes operating at temperature up to 580°C are made of alloys such as 23 weight

percent Cr, 1 percent Mo or even 9 percent Cr, 1 percent Mo. For still higher temperatures, the use of these low- or intermediate-alloy ferritic steels would require excessive wall thicknesses to withstand high pressures and to offset scaling, and their cost advantage would be lost. The highly alloyed materials - in particular, the austenitic stainless steels, "super alloys" and Ni-Cr-Fe alloys such as the Inconels and Incolloys - are therefore employed.

### Stainless steels

The addition of small amounts of selective elements such as copper or chromium to steel can impart substantial resistance to corrosion, so that some of the low-alloy steels have superior performance to plain carbon steel in atmospheric environments. True passivity in single-phase water systems, as achieved with the stainless steels, requires at least 12 weight percent of chromium as an alloying element. At least 20 weight percent chromium is required for true passivity in high-temperature gaseous oxidation. [Birks, 2006]

The stainless iron-chromium alloys are basically ferritic with a BCC crystal structure. They typically have chromium contents of 12-25 weight percent with about 1 percent manganese and silicon and up to 0.2 percent carbon, to which other elements such as the strong carbide-formers molybdenum, vanadium and niobium are added to enhance properties such as creep resistance. Like the carbon steels they can be heat-treated and conditioned, depending upon their content of carbon and other elements, to provide desired properties of strength, hardness and toughness. There are also grades that are commonly used in the martensitic condition, which typically contain 12-20 weight percent chromium, up to 1.0 percent carbon and often 1-2 percent nickel or up to 1.0 percent molybdenum.

The stainless steels used for corrosion resistance and for highest temperature service in power systems are the austenitic grades. For example, the cladding for the fuel sheaths in the carbon-dioxide-cooled AGR nuclear reactor, operating at temperatures up to about 650°C, is a 20 weight percent chromium, 25 percent nickel-niobium stainless steel. The Russian design of pressurized water reactor, the VVER, also uses austenitic stainless steel for the steam generator tubes operating below about 320°C. Austenitic steels have the FCC structure, which is stabilized at low temperature by the presence of nickel at concentrations between about 6 and 20 weight percent. Resistance to corrosion is again provided by the chromium, which is added at a concentration between 16 and 30 weight percent. For most power plant applications, stainless steels based on the common 18-8 or 18-12 (18 weight percent chromium and 8 percent or 12 percent nickel) grades are employed. In the designation of the American Society for the Testing of Materials (ASTM) they are types 304 and 320, respectively, of the general 300-series austenitic grades. Manganese is usually present at 2 weight percent and carbon at up to 0.2 percent, though special low-carbon grades with less than 0.03 percent carbon are available when a particular resistance to the deterioration of heat-affected regions such as welds by intergranular attack in corrosive media is required (see intergranular attack Section 4.4). The addition of small amounts of titanium or niobium to form the stabilized grades can also counteract such weld deterioration, which is caused by the removal of the protective chromium from solid solution within the grain boundaries by solid-state precipitation as chromium carbide over a specific temperature range – a process called sensitization. For resistance to pitting corrosion and to

improve creep resistance, molybdenum is added in the range of 2.0 to 3.0 weight percent to form type 316 stainless steel. It should be noted that the austenitic stainless steels cannot be heat-treated like the ferritic steels to improve strength or hardness; however, cold working can change the microstructure and form small amounts of martensite, for example, that change the properties and may even induce ferromagnetism. Annealing at high temperature will relieve the effects of cold-working.

### **2.2.3 Nickel Alloys**

For very high temperature applications (greater than 600°C or so) in power systems where strength, creep resistance and oxidation resistance are required, such as furnace or turbine fittings, or for environments where resistance to aqueous corrosion - particularly localised corrosion - is a major consideration, such as nuclear reactor coolant systems, nickel alloys may be employed.

Elemental nickel has the FCC crystal structure, which it tends to promote in its alloys - austenitic stainless steel being the prime example described above. Oxidation resistance of the nickel alloys is provided by chromium, which is present in the common alloys at concentrations between about 14 and 25 weight percent. For highly aggressive environments, such as strong acid solutions, the so-called "super alloys" with molybdenum additions up to 20 weight percent in alloys of the Hastelloy type, as produced by the Haynes International company, are effective and even higher levels (at about 30 percent with little or no chromium) produce the alloy Hastelloy B2 with superior resistance to concentrated hydrochloric and other reducing acids at all temperatures up to the boiling point. These materials may however have limited application in high-temperature environments in power systems.

**Table 2. Standard compositions of commonly used ferritic, martensitic and austenitic steels in CANDUs.**

Common designation	UNS #	chemical composition (wt%)								
		C-max	Fe	Cr	Ni	Mn	Mo	Si	P	Cu
Low-alloy steels										
A106 gr.B		0.3	Bal.	< 0.4	< 0.4	0.29-1.06	< 0.15	> 0.1	<0.035	<0.4
A106 gr.C		0.35	Bal.	< 0.4	< 0.4	0.29-1.06	< 0.15	> 0.1	<0.035	<0.4
Martensitic stainless steels										
403	S40300	0.15	Bal.	11.5-13	< 0.6	< 1.0		< 0.5	< 0.04	
410	S41000	0.15	Bal.	12.5		< 1.0			< 0.04	
Austenitic stainless steels										
304	S30400	0.08	Bal.	18-20	8-10.5	< 2		< 1.0	< 0.045	
304L	S30403	0.03	Bal.	18-20	8-12	< 2		< 1.0	< 0.045	
316	S31600	0.08	Bal.	16-18	10-14	< 2.0	2-3	< 1.0	< 0.045	
316L	S31603	0.03	Bal.	16-18	10-14	< 2.0	2-3	< 1.0	< 0.045	

A class of nickel alloys that should be mentioned here, even though they have not achieved wide use in thermal power systems but are extensively employed for gas turbine applications, is that of the super alloys, briefly mentioned above. They have outstanding strength, creep resistance and oxidation resistance at high temperature. Chromium concentrations around 20 weight percent provide their oxidation resistance, which may be enhanced by molybdenum at concentrations up to 10 percent in some cases. Grain-boundary properties, which affect creep, are improved by small additions of metals such as niobium, zirconium or hafnium while strength is imparted by additions of aluminium and titanium. The last two metals, usually present at levels of a fraction of a percent, strengthen the FCC crystal structure by precipitating with nickel as an intermetallic compound called gamma prime ( $\gamma'$ ). This precipitation hardening or age hardening process is carried out at temperatures approaching 900°C on material that has been quenched from solution treatment in a high-temperature region where all the constituents are in solid solution. A typical alloy of this type is Inconel X750, as produced by the International Nickel company, which contains 70 weight percent nickel, up to 17 percent chromium, up to 9 percent iron, about 1 percent niobium, 2.25 - 2.75 percent titanium and 0.4 - 1.0 percent aluminium. Alloy X750 in wire form has been used to form toroidal spacers to separate the hot pressure tubes from the surrounding cool calandria tubes. The alloy loses practically all its ductility under neutron irradiation but maintains sufficient strength to carry the necessary loadings. Compositions of some nickel alloys commonly used in nuclear power plants are shown in Table 3.

The most widespread application of nickel alloys in the nuclear industry is for the tubing of steam generators in water-cooled nuclear reactors of the CANDU or pressurized water reactor (PWR) type. In order to ensure resistance to stress corrosion cracking and general corrosion,

Alloy-400, a nickel-copper alloy based on Monel-400 (63-70 weight percent nickel, 28-34 percent copper, with 1-2 percent iron, as produced by International Nickel), was employed in early CANDU reactors. The more rigorous operating conditions in later CANDUs prompted a move to alloys with better resistance to general corrosion in a somewhat oxidizing water coolant, so Alloy-600 (72 weight percent nickel, 14-17 percent chromium and 6-10 percent iron) or Alloy-800 (30-35 percent nickel, 19-23 percent chromium with the balance of iron, which is still classed as a nickel alloy, even though the major constituent is iron) were employed. The last two materials, respectively based on Inconel and Incoloy as produced by International Nickel, are used widely in the PWRs, though Alloy-600 is being replaced with Alloy-690 (61 weight percent nickel, 30 percent chromium and 9 percent iron) as a material more resistant to cracking. It should be noted that the nickel-chromium alloys used for steam generator tubing improve their resistance to cracking when they are thermally treated to relieve the stresses imparted during tube forming.

**Table 3. Compositions of commonly used nickel alloys in nuclear power plants.**

Common designation	UNS #	chemical composition (wt%)									
		C-max	Fe	Cr	Ni	Mn	Mo	Si	P	Cu	Ti
600	N06600	0.15	6-10	14-17	Bal.	< 1.0	●	< 0.5	●	< 0.5	●
690	N06690	0.05	7-11	27-31	Bal.	< 0.5	8-10	<0.5	<0.015	< 0.05	●
X750	N07750	0.08	5-9	14-17	Bal.	< 1.0	2.8-3.3	< 0.5	●	< 0.5	2.25-2.75
800 NG	N08800	< 0.02	Bal.	19-23	30-35	< 1.5	●	< 1.0	●	< 0.75	0.15-0.6

## 2.2.4 Copper Alloys

Copper has an important engineering role in electrical equipment and conductors, stemming from its high electrical conductivity (second only to that of silver, which is about 10 percent higher). In addition, its high thermal conductivity, good mechanical properties and corrosion resistance in many environments make it an important material for heat exchangers in the power industry and elsewhere.

The pure metal melts at 1082°C and at all temperatures below this it has an FCC crystal structure as shown in Figure 1. It is readily worked and machined and has good resistance to atmospheric corrosion and corrosion in clean waters. For heat exchanger applications, however, it is alloyed most commonly with zinc - to form the brasses - or with nickel - to form the cupronickels. The alloys are harder and stronger than elemental copper and offer good resistance to aqueous corrosion - particularly in marine environments.

Zinc itself has an HCP crystal structure and it dissolves in copper to a maximum of about 37 weight percent at 500°C without changing the structure from FCC. The resulting solid solutions are in the  $\alpha$  phase, which is the basis of the  $\alpha$ -brasses. Zinc concentrations above the 37 weight

percent limit precipitate a second phase, the BCC  $\beta$  phase, which becomes the sole equilibrium phase between about 46 and 50 percent zinc. Above this limit another phase, the  $\gamma$  phase, precipitates but forms brittle alloys that are of little commercial utility.

The most widely used brass in the power industry is based on the single-phase 70-30 alloy (70 weight percent copper, 30 percent zinc), since this has the optimum combination of mechanical properties and corrosion resistance and is not subject to the problems of reduced ductility and difficulty of working experienced by the two-phase  $\alpha$ - $\beta$  or the single-phase  $\beta$  brasses. While the  $\alpha$ -brasses are easily formed into tubing etc., they tend to lose ductility with increasing cold work and must be annealed at high temperature to avoid stress corrosion cracking (known as season cracking) in service. Brasses are also susceptible in aqueous environments to a type of corrosion called dezincification, in which the alloy is transformed in its original shape to porous copper having little rigidity or strength. This phenomenon is stifled by as little as 0.04 weight percent arsenic, which is a standard additive to  $\alpha$ -brasses. A common material for heat exchangers and condensers is Admiralty brass, having 71 weight percent copper, 28 percent zinc, 0.02 to 0.06 percent arsenic and small amounts of lead and iron. Antimony and phosphorus are similar to arsenic in their corrosion inhibition of brass.

Nickel has a similar FCC crystal structure to that of copper, and the two elements are completely soluble in each other in all proportions. The resulting  $\alpha$ -phase solid solutions therefore have melting points between that of pure copper (1082°C) and that of pure nickel (1452°C). The cupronickels (so-called when the copper is the major constituent) are tough, readily worked and have a high corrosion resistance. Alloys based on 70 weight percent copper and 30 percent nickel, the 70-30 cupronickels, find widespread use in heat exchangers for sea water service, when additions of iron and manganese to about 2 percent provide extra resistance to erosion-corrosion. The 90-10 cupronickels have better thermal conductivity than the 70-30 alloy and are more resistant to aqueous corrosion at higher temperatures, so they have been commonly used in feedwater heaters in steam-raising systems.

### 2.2.5 Titanium Alloys

Pure titanium has an HCP crystal structure (the  $\alpha$  phase) at temperatures up to 884°C, where it transforms to the BCC  $\beta$  phase, which is stable up to the melting point of 1677°C. Alloying elements stabilize one phase or the other. Aluminum, carbon, oxygen and nitrogen, for example, stabilize the  $\alpha$  phase and raise the  $\alpha$ - $\beta$  transition temperature, whereas copper, chromium, iron, molybdenum and vanadium lower the transition temperature and may even stabilize the  $\beta$  phase at room temperature.

The principal titanium alloys are therefore of three types: alpha or near-alpha, alpha-beta and beta. Their high strength-to-weight ratio (especially of the alpha or near-alpha and alpha-beta alloys) has put them in high demand in the aerospace industry, while in the power industry the exceptional resistance to corrosion in a wide range of corrosive waters - particularly sea water - has made titanium an important material for condenser tubes and plate heat exchangers.

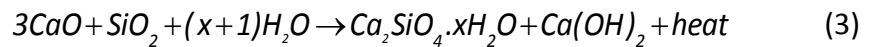
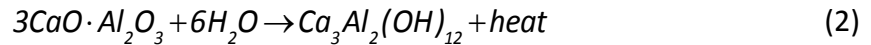
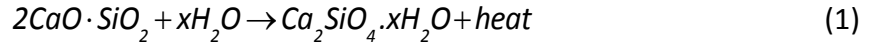
Titanium is actually a very reactive metal and must be melted and machined with care. Its resistance to corrosion is afforded by the thin, protective layer of oxide ( $\text{TiO}_2$ ) that spontaneously forms in air to produce an effective barrier against the environment, thereby putting titanium in the class of passive metals. The rather specialized metal refining and component manufacturing process for titanium tubing at one time made the material an expensive proposition for condensers. The growing demand for titanium products, however, has had the effect of lowering the price relative to competitive materials - especially the copper alloys and steels. Also, the development of seam-welded tubing suitable for condenser service and the fact that no thickness allowance need be made for corrosion on the tube wall makes titanium an attractive alternative.

The titanium used mostly in condenser applications is the commercially pure material, which is therefore an alpha-phase material. It exists in five grades distinguished by their impurity content. Thus, the maximum amounts of carbon, nitrogen, hydrogen, iron and oxygen are specified for each grade at levels of the order of 0.01 to 0.1 weight percent, and each grade has particular mechanical properties. Titanium condenser tubing is relatively immune to corrosion in salt or brackish water and in all types of polluted water. Marine organisms stick to its smooth surface with some difficulty and surfaces that do foul or silt are not susceptible to pitting or crevice corrosion. On the condensing steam side of the tubes used for power plant condensers, there is no effect on titanium from common gases such as ammonia, carbon dioxide or oxygen. In fact, the main concern with the use of titanium for condenser tubes is that less noble components of the condenser may suffer galvanically-accelerated corrosion and must be protected either cathodically or by coating or both. It must be borne in mind that in aqueous service the metal absorbs hydrogen readily, so that its exposure as the cathodic component of a metallic couple can promote degradation as the titanium-hydride is formed and the material becomes embrittled.

### 2.2.6 Concrete

Concrete is an inorganic composite consisting of a coarse aggregate of gravel, crushed rock or slag and a fine aggregate of sand, all held together with a cement. Angular particles or rock fragments are preferred to rounded ones for the aggregate because they tend to interlock and produce a more bonded and therefore stronger structure, although they have more surface defects that can initiate cracks or voids. The larger the aggregate the better in order to minimize the defects, bearing in mind that the size of the particles or fragments should be no more than ~20% of the structure's thickness. The aggregate material can be tailored to the requirements of the structure. Lightweight concrete incorporating steel-making slag as aggregate, for instance, is a better thermal insulator than one incorporating normal silica-based rock, and heavy concrete incorporating dense mineral aggregate such as ilmenite, barytes or magnetite or even metal shot is used for radiation shielding. Ideally, the sand is a silica-based mineral with particle size 0.1 – 1.0 mm. It partially fills the spaces between the coarse aggregate and reduces the porosity of the final concrete, in turn reducing the tendency to disintegrate during alternate freeze-thaw cycles. The cement is a mixture of fine mineral particles that sets and hardens after being made into a paste with water. The most common type of cement is Portland cement, named after the cliffs at Portland in England, which the hardened material resembles. Portland cement is a type

of hydraulic cement, i.e., one that hardens upon reaction with water. It is a mixture of calcium silicate (conveniently designated as 60-65% CaO and 20-25% SiO<sub>2</sub>), iron oxide and alumina (7-12%). Adding water hydrates the mixture to produce a solid gel, releasing heat as it does so. The main chemical reactions can be generalized to:



The hardened cement binds the aggregate particles together, so there must be enough cement added to coat all of the particles completely if a firm composite is to be obtained. A typical cement proportion is 15 vol% of total solids. Both the time to harden and the strength of the final concrete depend on the composition of the initial mixture; a rapid-setting concrete generally is weaker than a slow-setting one. Complete curing is attained after 28 days or so, when concrete reaches its maximum compressive strength.

Like other ceramic-based materials, concrete is strong in compression but weak in tension, so for most construction purposes it has to be strengthened. Reinforced concrete has steel rods (“rebars”), wires or mesh introduced into the structure to take the tensile loads, while the concrete supports the parts under compression. Such a combination is effective for components undergoing bending forces. In prestressed concrete the reinforcing steel is pulled in tension between an anchor and a jack while the concrete is poured and cured. After the concrete has set, the external tension on the steel is removed and as it relaxes the forces are transferred to the surrounding restraining concrete, placing it in compression. The component can now resist higher tensile or bending forces. Post-stressed concrete also has induced compressive stresses, but they are imposed by running steel cables or rods through tubes set in the structure and pulling and maintaining them in tension after the concrete has hardened. Reinforced concrete has many applications in nuclear reactor construction – building foundations, primary containment and shielding, supports for large components such as steam generators, etc. Concrete containment buildings are pre- or post-stressed, and for the LWRs are lined with steel plate. Existing CANDU containment buildings are lined with epoxy.

Concrete structures undergo various modes of degradation. Rebar in civil installations, typically bridges and road overpasses, corrodes in contact with aqueous solutions such as road salt and in time can cause serious deterioration of the structure. Pre- and post-stressing steel can also rust and lose strength and over time the compressive stresses may relax. The concrete itself may be attacked; chlorides, nitrates and sulphates react with the cement and cycles of freezing and thawing can cause cracking. An insidious mode of degradation for concretes with aggregate containing silica in a non-crystalline or glassy form is the co-called alkali-aggregate reaction (AAR). This is an internal process whereby alkaline constituents of the cement react over time with the silica to form a hydrated calcium silicate. This compound has a larger volume than its precursors and the resultant swelling causes the structure gradually to spall and crack. The hydro-electric dam at Mactaquac on the St. John river in New Brunswick has a particularly pernicious form of this degradation. The concrete swelling puts such severe compressive forces on the structure, which is firmly anchored between rock abutments, that the stresses have to be

relieved periodically by sawing vertically through the dam from top to bottom – a process that can continue only for about another decade. The plinth supporting the turbine at the Gentilly-2 CANDU is cracking because of this form of degradation. Concrete used as radiation shielding around a nuclear reactor relies on its water content to maintain not only its strength but also its effectiveness for stopping neutrons. Over time, the absorption of radiation and the resulting heating can lead to dehydration, involving water both bound chemically with hydrous minerals and free as excess molecules. To minimize these losses, reactor shielding structures are continuously cooled, often with cooling water pipes embedded in the structure.

### 2.2.7 Polymers

Polymers for industrial or domestic consumption are generally called plastics. Because of their ease of manufacture and formation, their physical and chemical properties and their low cost they have a huge number of applications. The transparency of several types makes them useful as substitutes for glass whilst the elasticity of others puts them in the class of elastomers. They can be produced as homogeneous material or as both the matrix and the fibre reinforcement for composites. In reactor systems they are used for electrical insulation, coatings, seals, etc. and occur in a myriad of common articles such as textiles, containers, tools, etc.

Most polymers, and the ones discussed here, are composed of “giant” molecules consisting of chains of simpler units bonded together. They are usually organic carbon-based compounds, although some are inorganic, based on silicone Si-O units. Molecular weights can range from  $10^4$  to  $10^6$  g/mol or higher. A linear polymer has its molecules as single strands in a tangled arrangement, rather like a portion of spaghetti. In a branched polymer, each “spaghetti” strand has one or more shorter strands branching off. Linear or branched polymers can be cross-linked, whereby atoms in individual strands are strongly bonded covalently to atoms in other strands, either directly or via linking atoms.

Thermoplastics are composed of linear or branched molecular strands that are weakly connected to each other by van der Waals bonds and that can be partially separated or untangled by applying tensile stress. Thermoplastics therefore are ductile and deform plastically. When heated they at first soften and then melt, making them easily moulded into useful articles and readily recycled. Polyethylene is a common example of a thermoplastic. By contrast, thermosetting plastics have their linear or branched molecular strands strongly bonded covalently to each other in a rigid, three-dimensional network. They are therefore stronger than thermoplastics but more brittle. On heating, they do not melt but decompose, making them difficult to recycle. Polyurethanes are an example of a thermosetting plastic. Elastomers are thermoplastic or lightly cross-linked polymers that have their molecular strands in a folded or coiled configuration. Under stress the molecules deform reversibly, rather like a spring, so that the original form is regained when the stress is relaxed. Natural rubber is the prime example of an elastomer which can be stretched elastically to >200%. The soft, thermoplastic latex from the rubber tree is made into useful rubber by “vulcanising”, involving reacting it with sulphur to cross-link the highly folded molecular strands. Depending on the degree of vulcanisation, a tougher and more elastic material is formed, one that does not soften and become sticky when heated to moderate temperatures. Low (1 – 3%) sulphur contents form soft commercial rubber, while high (23-



It is noteworthy that polytetrafluoroethylene (PTFE – or the DuPont trade name Teflon®), a most useful product in many domestic and industrial applications because of its non-stick and low friction properties, is the most severely affected by radiation in the list in Table 4 (in any case, its use in reactor systems is proscribed because it tends to release fluorine species as it degrades, and fluorine is particularly damaging to zirconium and its alloys).

## 3 CANDU Process Systems and their Materials

### 3.1 Major Process Systems

Diagrams of the various systems are presented in other chapters. The materials of construction of those systems are listed here. Their operating experience has been detailed by Tapping (2008).

#### 3.1.1 Primary Heat Transport System

The primary heat transport system consists mainly of the in-core fuel channels connected to the steam generators by a system of feeder pipes and headers. It has a purification system for the heavy water (isotopic purity  $\geq 95.5\text{wt}\%$ ) and is connected to a pressurizer.

The fuel channel components in contact with the heavy water primary coolant comprise the pressure tubes of Zr-2.5%Nb, the end-fittings of type 403 stainless steel, the liner tubes of type 410 stainless steel, the shield plugs of ductile iron and the seal plugs of Cr-Fe stainless steel. The fuel bundles are of elements sheathed with Zircaloy-4 that are separated by spacers of Zircaloy-4 that are resistance-welded to the end-plates, which are also made of Zircaloy-4. Bundles sit inside the pressure tubes on bearing pads of Zircaloy-4 which, like the spacers, are attached to the elements with a braze of Zr-Be.

The feeders and headers are made of carbon steel. Originally, when a low cobalt content was specified to minimize radiation-field build-up around the PHT circuit, a low-chromium material (A106 grade B with  $\sim 0.02\text{wt}\%\text{Cr}$ ) was selected. As described in Section 4.2 of this chapter and in Section 3.2 of Chapter 15, this gave rise to flow-accelerated corrosion (FAC) of the feeders at the reactor outlet. Replacement outlet feeders are specified as A106C with a chromium level of about  $0.3\text{wt}\%\text{Cr}$ , which, based upon extensive laboratory testing, should be enough to extend the life of the outlet feeders by about 50% and significantly reduce system fouling from transported corrosion products. A degradation phenomenon in some outlet feeders before replacement was a type of cracking, which occurred only at the Point Lepreau CANDU-6. Incidences of feeder cracking at other CANDUs have been extremely low – confined to one repaired field weld – making the Point Lepreau experience unique and rather mysterious. By 2005, nine feeders had been removed because of deep cracks from the inside surfaces, in some cases they were through-wall (Slade and Gendron, 2005), and a total of 12 feeders had been removed and replaced up to the time of the refurbishment shut-down that began in 2008. Cracks were all in the first and/or second tight-radius bends downstream of the fuel channel outlet, where residual stresses were high and where FAC was prevalent. Detailed examination revealed extensive shallow cracks on the outside surfaces also, and these outside-surface cracks were

found to be widespread in feeder bends across the reactor face. The cracking mechanism was not conclusively identified before Point Lepreau was shut down for the refurbishment, which included replacement of the feeders with the A106C material mentioned above and with stress-relieved bends. However, it was postulated that the inside-surface cracks possibly originated from stress-corrosion cracking caused by slightly oxidizing conditions at the reactor outlet due to insufficient suppression of radiolysis and exacerbated at reactor start-up, especially if air ingress had occurred. The outside-surface cracking was possibly low-temperature creep cracking, facilitated by atomic deuterium diffusing through the metal lattice due to FAC (Slade and Gendron, 2005).

The purification is a feed-and-bleed system taken off the connection between the coolant loops or, at Bruce A (which has only one primary loop) directly off the reactor headers. It has heat exchangers with tubes of nickel alloy (e.g., Alloy-600 or Alloy-800) and vessels such as the ion-exchange columns of 300-series stainless steel. The pressurizer, also taken off the connection between the coolant loops, is a carbon-steel vessel with immersion heaters clad with nickel alloy.

The steam generators are tubed with nickel alloy – Alloy-400 at Pickering, Alloy-600 at Bruce and Alloy-800 at the CANDU 6s and Darlington and the refurbished units at Bruce (Units 1 & 2). The replacement units at Bruce, like all the other CANDU steam generators except the original designs at Bruce A, are of the “light-bulb” design (see Figure 17 in Chapter 8) with the steam separator and dryer separate for each unit above the tube bundle (each original Bruce A design has four steam generators connected to an integral steam drum at each end of the reactor). The tube sheets in the primary heads are clad with the tube material, but the heads themselves are carbon steel. The divider plates in the steam generator heads have been replaced with stainless steel to eliminate FAC. All the steam generators except those at Bruce have integral preheaters, but at Bruce the preheaters are separate heat exchangers of carbon steel with tubes of Alloy-600 and tube sheets in contact with the primary coolant clad with the same material (the Bruce preheaters remove heat from the primary coolant serving the inner core fuel channels, which run at a higher power than the outer core ones).

### **3.1.2 Secondary Heat Transport System**

The secondary coolant system consists of the shell side of the steam generators, fed with light-water coolant from the condenser and feed water train and supplying steam to the turbine and thence back to the condenser. CANDUs have been following a policy of eliminating copper alloys from the circuit to avoid corrosion problems from carry-over to the steam generators. The only components remaining with copper alloys are brass-tubed condensers at Gentilly 2 (currently shut down and due for decommissioning), as listed below, although it is of note that Pickering changed its condensers from brass to stainless steel because of release of copper to Lake Ontario.

As mentioned above, steam generator tubing is Alloy-400 at Pickering, Alloy-600 in the original units at Bruce – Alloy-800 in replacement units and at Darlington and the CANDU 6s. The tube supports at Pickering A are lattice bars of carbon steel and at Pickering B are broached plates of carbon steel; at Bruce the original supports are broached plates of carbon steel but, like Darling-

ton and the CANDU 6s (except Embalse, Point Lepreau and Wolsong 1), the replacement units have lattice bars of type 410 stainless steel. Embalse has broached plates of carbon steel, Point Lepreau has broached plates of type 410 stainless steel and Wolsong 1 has lattice bars of Alloy 600. Steam generator shells, shrouds, etc. are of low-alloy/carbon steel.

The feedwater and steam cycle piping is generally carbon steel, although some regions of the system susceptible to flow-accelerated corrosion, such as piping carrying two-phase steam-water mixtures or highly-turbulent feedwater, may have alloy steel or even stainless steel.

All CANDUs except Embalse have a deaerator in the feed water train. These, the high-pressure feedwater heaters and the moisture-separator/reheater in the steam circuit are made mostly of carbon steel, although stainless steel may be employed for some reheater tubes. The low-pressure feedwater heaters are made of stainless steel.

The condensers at Point Lepreau and the Qinshan CANDUs are tubed with titanium since they draw from sea water while the Embalse plant continues to use Admiralty brass (with stainless steel for the outer tubes of the bundles). The remaining CANDUs use Type 304 stainless steel as their condenser tubes, Bruce units 1 & 2 being the most recently converted during their refurbishment project that was completed in 2012.

### 3.1.3 Moderator

The moderator system is the piping and components containing and processing the heavy water moderator (isotopic purity  $\geq 99.75\text{wt}\%$ ). It includes the cover gas system containing the helium cover gas and maintaining its content of deuterium and oxygen (formed by heavy-water radiolysis in the reactor) at safe levels of  $<2\text{wt}\%$  via a catalytic recombiner.

All reactors have a calandria vessel made of type 304L stainless steel and calandria tubes made of Zircaloy-2. Most of the rest of the circuits (including the heavy water expansion tank) are of stainless steel, except the heat exchangers, which are nickel alloy – primarily Alloy 800.

## 3.2 Ancillary Process Systems

### 3.2.1 Condenser Cooling Water

CANDU condensers are cooled with whatever natural water source is available – sea water at coastal sites or fresh/brackish water at riverside or lakeside sites. Water is drawn into the system through a steel screen arrangement to remove coarse debris, pumped through a circuit of concrete ductwork and steel piping to the condenser, then discharged back to the source. No CANDU to date has employed cooling towers to enable recirculation of condenser cooling water.

The condenser tubing materials have already been listed above. Like the condenser shells, the inlet and outlet “water boxes” are of carbon steel and they may be cathodically protected from galvanic corrosion caused by contact with tube sheets of more noble metals.

### 3.2.2 Recirculating Cooling Water (RCW)

This system of purified water kept usually at high pH (typically adjusted using the AVT strategy of the steam cycle) and low oxygen with hydrazine additions cools components such as the moderator heat exchangers. It comprises its own heat exchangers of nickel alloy – normally Alloy 800 – and carbon steel piping fed directly from the local water source.

### 3.2.3 Shield Tank

The shield tank encloses the calandria circumference, providing shielding and cooling for the reactor. In the early reactors it is a water-cooled carbon steel vessel but in the CANDU 6 it is the concrete vault filled with water. The end shields are water-cooled tanks filled with  $\frac{3}{8}$ "-  $\frac{1}{2}$ " diameter carbon-steel balls that provide shut-down biological shielding for the reactor faces and support for the fuel channel assemblies. They are made of type 304L stainless steel and have lattice tubes (to accommodate the fuel channel end-fittings) of the same material. Like the main shield tank, they are filled with  $\frac{3}{8}$ "-  $\frac{1}{2}$ " diameter carbon-steel balls. Note that the Pickering reactors have cooled steel slabs as end shields rather than water-cooled tanks.

The purified water, maintained at high pH with lithium hydroxide, is circulated through heat exchangers tubed with nickel alloy or even copper alloy, where it is cooled by plant service water (RCW).

### 3.2.4 Spent Fuel Bay

The spent fuel bay is the swimming-pool arrangement for accepting and storing spent fuel under water directly from the reactor. About ten-year's accumulation (at ~80% capacity factor of the plant output) of fuel bundles can be stored with about 4m of water above. The water cools the bundles and provides biological shielding. There is an intermediate bay for handling and temporary storage. The construction is reinforced concrete lined with epoxy-coated fiberglass and with a stainless steel floor.

### 3.2.5 Emergency Cooling

The emergency core cooling system (ECC) is a light-water system designed to supply cooling water to the reactor core via the primary coolant system emergency injection. It is triggered by a loss in pressure following a LOCA (loss-of-coolant accident) and for later reactors with individual containment buildings, is supplied initially from the ECC water tanks which are located outside the containment. For high-pressure operation as occurs with a small leak, the water is injected into the primary coolant headers by automatically pressurizing the ECC tanks with nitrogen (the loop is automatically isolated from the other one). As the system pressure drops, the ECC pumps start and stored water is then injected into the headers from the dousing tank, which is below the roof slab. During these phases, the heat sink is the steam generators. Finally, when the dousing tank is empty and the system pressure has dropped even further, collected water is pumped into the system from the sump via the ECC heat exchanger, which is cooled with service water. This phase is designed to continue indefinitely. The multi-unit stations with a vacuum building have the ECC storage as the dousing tank below the roof slab of the vacuum building.

The dousing tank below the roof slab is made of reinforced concrete and the piping system of carbon steel and stainless steel. In the later reactors the shell-and-tube ECC heat exchangers to reject heat to the outside are alloy-tubed but early designs used titanium plate-type heat exchangers.

### **3.3 Supporting Structures and Components**

#### **3.3.1 Containment**

In the four-unit CANDUs at Darlington and Bruce A and B, the reactor of each unit is contained within a reinforced concrete vault, which extends to shielded rooms above containing the steam generators, heat transport pumps and reactivity drive mechanisms. Main steam piping exits the containment for the turbine building. Openings in the floor of the vault allow entry of the fuelling machine, which serves all four units via a duct running below grade for the length of the station and connecting to a fuel handling facility. The overall building for each unit has a flat, steel roof.

The four-unit CANDUs at Pickering A and B, like the CANDU 6 reactors, each have the reactor, steam generators, etc., in a separate containment building of pre-stressed, post-tensioned concrete with a domed roof. The building is lined with epoxy, but future designs could incorporate a steel liner. The main steam pipes exit the containment directly for the turbine building.

#### **3.3.2 Vacuum Building (Multi-unit Plants)**

Bruce A and B and Darlington each have the four reactor containments separately connected to a normally sealed building that is kept at about 7kPa absolute pressure. At Pickering, the eight units at the A and B sites are connected to one such vacuum building. In the event of an over-pressure in a reactor containment, isolation valves connecting that reactor with a concrete duct running to the vacuum building open and the atmosphere of the containment is vented. A spray from the ECC storage in the vacuum building roof condenses any vapour.

The vacuum building is constructed of reinforced concrete. It is supported inside with an arrangement of columns and beams that also hold up the ECC storage tank and the vacuum chambers.

#### **3.3.3 Fuelling Machine**

Each CANDU reactor is served by two fuelling machines, with one machine connecting to each end of a fuel channel that is to be refueled. A machine has a rotating magazine to hold fuel and channel seals and plugs, a snout assembly to lock onto the channel and a ram assembly to remove, store and replace channel seals, plugs and fuel bundles. Figures 10 – 12 in Chapter 8 show the arrangement of the fuelling machine.

The machines simultaneously clamp onto the end-fittings of a channel, unlock, remove and store the seal plugs, remove and store the shield plugs then push new fuel bundles into the pressure tube from one end and remove and store spent fuel bundles from the other end, replace the shield plugs and finally replace and lock the seal plugs. During the operation the machine is in contact with the primary coolant at pressure and sustains a flow of heavy water from the PHT supply tanks. The seal plug sealing faces must be maintained in good condition to prevent expensive heavy water leaks.

Fuelling machines are large pieces of equipment comprising many components that remotely perform a complex series of tasks. They are made of many engineering materials. Of note are the mechanical bearings that support the rotating magazine, which have traditionally been made of the extremely hard-wearing cobalt alloy, Stellite®. This has been responsible for a significant component of out-core radiation fields, since even very small releases of cobalt to the primary coolant during a refuelling operation may give rise to the production of  $^{60}\text{Co}$  in the reactor core, and this distributes around the circuit and contaminates out-core components, particularly at the reactor faces and in the steam generator heads. Recent research is identifying alternative materials for the bearings such as silicon nitride (see for example Qiu, L., 2013). Additionally, activation products of antimony (primarily Sb-124) originate from bearings in the heat transport pumps and as impurities in steel and may contribute significantly to the overall activity levels throughout the primary heat transport circuit.

### 3.3.4 Fuel

The fuel materials in contact with the primary coolant, viz. the element sheaths, end plates, bearing pads, spacers and the braze attaching the appendages to the sheath have already been described. The fuel pellets themselves within a sheath are of high-density, sintered  $\text{UO}_2$  of natural isotopic content (0.7%  $^{235}\text{U}$ ) and the inside surface of the sheath is coated with a thin layer of graphite to reduce sheath-pellet interactions (the CANLUB system). The standard bundle is of 37 similar elements; however, more-efficient designs such as the CANFLEX® bundle with 43 elements of different diameters have been proposed; thus, for future applications, the Advanced CANDU Reactor employs low-enriched uranium (LEU) fuel of  $\text{UO}_2$  with 3-4%  $^{235}\text{U}$  in a CANFLEX®-type bundle with a central element containing a neutron absorber. Note that the flexibility of the CANDU system makes it suitable for a wide variety of fuel materials, and trials with thorium, recovered uranium (from reprocessing of LWR-type fuel) and plutonium mixed-oxide (with uranium) have been carried out successfully.

### 3.3.5 Reactor Control Mechanisms

Liquid zone controllers are vertical thimble tubes of type 304 stainless steel attached vertically to the top of the calandria with zone control tubes of Zircaloy extending downwards into the moderator between the calandria tubes. They control reactivity during normal operation. Six of them per reactor contain among them fourteen compartments of circulating light water as the absorber, and the amount of absorber can be controlled by adjusting an overpressure of helium in each compartment and the inlet flow rate.

There are mechanical adjuster rods (21 in the CANDU 6s), also inserted vertically into the moderator, to act as neutron absorbers. They are tubes of stainless steel or Zircaloy containing “shim rods” of steel/cadmium or cobalt that are normally fully inserted to flatten the flux profile but can be withdrawn mechanically via motor-driven winches (sheaves) and cables as override for xenon poisoning following reactor shutdown or a power reduction.

Shut-off rods and mechanical control absorbers are of similar design, penetrating the calandria vertically between the calandria tubes in similar fashion to the adjuster rods. Each employs a cable, winch and clutch to hoist, hold or release an absorber tube containing cadmium as a neutron absorber. They are normally parked in thimbles above the calandria but can be driven vertically downwards into the core to reduce reactivity through perforated guide tubes of Zircaloy that are anchored at the bottom of the calandria. Shutdown System #1 comprises 28 such assemblies arranged throughout the reactor; they release their rods by de-energising the clutch and drive them into the core by spring-assisted gravity to achieve rapid power decrease. Four other assemblies can be used for reactor control to supplement the liquid zone controllers. They are normally parked out of the core but are driven in at variable speeds as required to reduce reactor power.

## 4 Corrosion and Material Degradation in Nuclear Reactor Systems

As described above and elsewhere in this text, a nuclear reactor is a complex system of different connected materials that must behave optimally in unison to ensure the safe and efficient operation of the plant. Even under the strictest chemistry control practices and careful plant operation, the corrosion and subsequent degradation of the plant components are the inevitable consequences of thermodynamics; the metals that make up the pipes, valves, fittings and vessels all tend to revert back to their thermodynamically stable state – usually an oxide, haematite ( $\text{Fe}_2\text{O}_3$ ) for example, the basis of rust on iron and steel. In some cases, the degradation of system components is exacerbated by vibration, fatigue or fretting or by the interaction with high-velocity coolant creating flow-accelerated corrosion (FAC); in all cases, component lifetimes are shortened. Thus, knowledge of the basic forms of corrosion is a prerequisite to understanding the materials selection and chemistry requirements of CANDUs.

### 4.1 General Corrosion

Metals that are in every-day use for engineering applications are fundamentally unstable. They tend to react with their environment to assume a more stable thermodynamic state, which in the coolant systems of nuclear reactors is normally an oxide. General corrosion is the term for attack that is spread more or less uniformly over the entire component surface; it is driven by an electrochemical reaction in the case of ionic environments such as molten salts or aqueous coolants, or by a chemical reaction in the case of non-ionic coolants such as gases like carbon dioxide. (Note, however, that any oxidation is strictly speaking electrochemical, since it is a chemical reaction involving the transfer of electrons.) The metal thins gradually and may fail if left without being inspected for any length of time, although the rates of such corrosion are low and are generally predictable from tabulated data. Components are designed with adequate

thickness (incorporating a “corrosion allowance”) that will last for the desired lifetime; failures are rare.

#### 4.1.1 General corrosion in gas-cooled systems

As an example of a direct chemical oxidation, consider the alloy steel Fe-9%Cr as the boiler-tube material in Advanced Gas-Cooled Reactors (AGRs). In the CO<sub>2</sub> coolant at 580°C this material corrodes uniformly, forming a duplex film of the oxide Fe-Cr spinel (based on iron chromite, FeCr<sub>2</sub>O<sub>4</sub>) overlaid with the inverse spinel magnetite (Fe<sub>3</sub>O<sub>4</sub>). Spinels have a crystal structure in which the unit cell contains 32 oxide ions in a face-centred cubic arrangement and 24 metal ions dispersed in the interstices to neutralise the charge. The interstices comprise 64 sites with tetrahedral symmetry and 32 sites with octahedral symmetry. In so-called normal spinels, the eight divalent metal cations (Fe<sup>2+</sup> in the example of FeCr<sub>2</sub>O<sub>4</sub>) are in tetrahedral sites and the 16 trivalent cations (Cr<sup>3+</sup> in FeCr<sub>2</sub>O<sub>4</sub>) are in octahedral sites. In inverse spinels, the divalent cations (Fe<sup>2+</sup> in Fe<sub>3</sub>O<sub>4</sub>) are distributed along with half the trivalent cations (Fe<sup>3+</sup> in Fe<sub>3</sub>O<sub>4</sub>) in octahedral sites, while the remaining trivalent cations are in tetrahedral sites. The relative stabilities of the normal and inverse spinel lattices influence the extent to which magnetite can incorporate Cr<sup>3+</sup> ions and chromite can incorporate Fe<sup>3+</sup> ions.

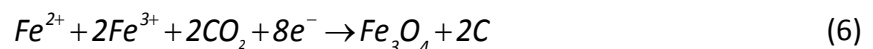
The mechanism for the formation of the duplex oxide film on the AGR steel has been postulated to be the direct reaction of metal with CO<sub>2</sub> that diffuses through pores and microchannels in the growing oxide [Kofstad, 1985]. For example:



The carbon is distributed through the oxide and may carburise the metal. The development of the oxide porosity is governed by stresses created at the metal-oxide interface (M-O) by the difference between the density of the oxide and that of the metal (quantified as the “Pilling-Bedworth” ratio, which is defined as the ratio of the volume oxide formed to the equivalent volume of metal consumed; it is greater than unity for the common transition metals). We note, however, an alternative mechanism [Taylor et al., 1980], whereby corrosion is controlled by the protective nature of the inner layer; thus, the magnetite forms at the oxide-coolant interface (O-C) via direct chemical reaction with CO<sub>2</sub> of Fe that has migrated through the oxide:



although the details will involve reactions with diffused ionic species:



The kinetics of general corrosion governed by the increasing protection afforded by a continuously-thickening oxide film are often described by a parabolic expression, derived from the principle that diffusion rate, and therefore corrosion rate and oxide film growth rate (dm/dt), is inversely proportional to film thickness (m):

$$\frac{dm}{dt} = \frac{k}{m} \quad (7)$$

which integrates to:

$$m^2 - m_o^2 = kt \quad (8)$$

where  $m_o$  is the initial film thickness. Modifications of (8) such as (9) are occasionally quoted:

$$m = m_o + kt^{0.5} \quad (9)$$

CANDU reactors have two main gas systems, although several ancillary systems also use inert cover gases to help prevent corrosion and maintain safety envelopes. The two main gas systems include the moderator cover gas system (already described) and the annulus gas system (AGS). The AGS circulates  $\text{CO}_2$  through the annulus between the calandria tube and its companion pressure tube. The system is continually monitored for moisture by dew point measurements as a warning of a leak from the PHT system or from the calandria end shield joint. Deuterium produced from the corrosion of the pressure tube on the PHT-side, diffuses into the AGS forming heavy water vapour when combined with oxygen present in the  $\text{CO}_2$  so the system needs to be regularly purged to reduce the moisture content. The oxygen added to the  $\text{CO}_2$  in the AGS also performs an important role of oxidizing the outside of the pressure tube. By oxidizing the outside pressure tube surface it helps to maintain a barrier to the ingress of deuterium into the pressure tube and promotes oxide formation on the X750 garter-spring spacers.

#### 4.1.2 General corrosion in water-cooled systems

Examples of electrochemical reactions are provided by the general corrosion of metals in water. Thus, carbon steel in contact with high-temperature water develops protective magnetite films according to the overall scheme:



The carbon steel feeders in CANDU primary coolant corrode accordingly, except that the coolant is  $\text{D}_2\text{O}$  rather than  $\text{H}_2\text{O}$  and deuterium rather than hydrogen is evolved. Mechanistically, (10) can be regarded as two half-reactions, the anodic or oxidation process:



and the cathodic or reduction process:



The half-reactions occur simultaneously and at the same rate. According to the classic Wagner-Traud theory [Wagner and Traud, 1938] it is postulated that the anodic sites on the metal, where metal ions dissolve (reaction (11)), are separate from the cathodic sites, where electrons are discharged, oxide ions form and hydrogen is released (reaction (12)). The electrons are transported between the sites and the metal ions and oxide ions interact and precipitate as magnetite. Clearly, for the oxidation to be uniform, the sites must be mobile across the surface.

In reality, it is understood that in high-temperature water the oxidation at the M-O produces ferrous ions according to:



and that the hydrogen is produced in the accompanying reduction:



where H is in the form of hydrogen atoms that migrate through the metal. It is important to note that if dissolved oxygen is introduced into neutral or alkaline water, reaction (14) is replaced by the more favourable reaction (15):

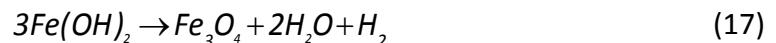


and hydrogen production ceases.

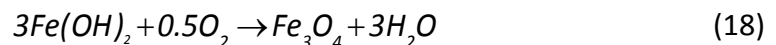
The ferrous ions and hydroxide ions from (13) and (14) or (15) interact to form soluble ferrous hydroxide:



but this oxidises and precipitates as magnetite according to the Schikorr reaction [Schikorr, 1928]:



Again, if oxygen is present, the oxidation of ferrous hydroxide proceeds via the more favourable:



There is only room at the M-O (metal-oxide interface) for about half of the ferrous hydroxide to precipitate there as inner-layer magnetite; the other half, along with any hydrogen molecules generated at the M-O by (17), diffuse through the developing magnetite film to the O-C (oxide-coolant interface). There, if the coolant is reducing and saturated in dissolved iron as in the carbon steel inlet feeders of CANDUs, it precipitates as outer-layer magnetite according to (17);

the molecular hydrogen is then dispersed in the bulk of the flowing coolant. In the presence of dissolved oxygen, the outer layer precipitates according to (18) and the magnetite film develops completely without the evolution of hydrogen. In time, it may itself oxidise to the Fe(III) oxide haematite:



and if the conditions are oxidising enough haematite may be formed directly without the intermediate formation of magnetite.

The duplex films of magnetite generally consist of a fine-grained inner layer of particles ten or so nanometres in size, overlaid with crystallites of sizes up to about ten micrometres. The outer layer crystallites are generally faceted octahedra, obviously grown from solution (see Figure 5 and 6).

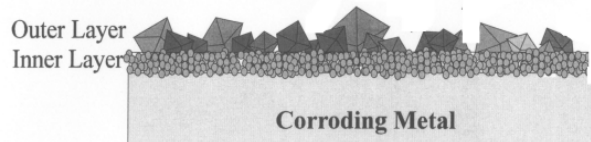


**Figure 5. Schematic Cross-Section through Magnetite Film on Carbon Steel [Lister, 2003]**

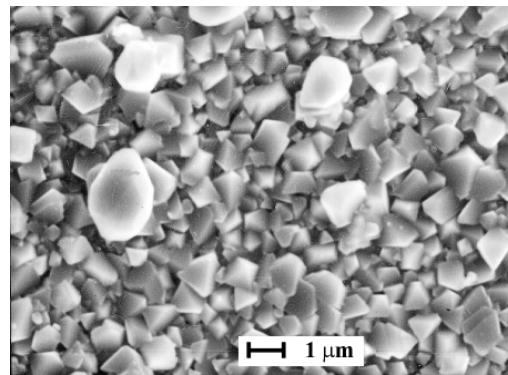


**Figure 6. Scanning Electron Micrograph of Magnetite Film formed on Carbon Steel during an 1100-h Exposure in High-Temperature Water [Lister, 2003]**

The general corrosion of the higher alloyed materials in widespread use in water reactor systems, such as the stainless steels and nickel alloys, also leads to the development of duplex oxide films. The oxide layers are generally thin and compact, conferring a high degree of corrosion resistance. The precise compositions of the oxides depend on the coolant chemistry, particularly the oxidising propensity. In general, it is the inner layers that “passivate” the alloy; these are based on the normal spinel  $FeCr_2O_4$ , which has a very stable lattice structure and a low solubility in the chemically reducing coolants of the pressurised water reactors (PWRs) and CANDUs [Lister, 1993]. Variants of the iron chromite structure contain elements arising from other alloy constituents such as nickel, viz.  $Ni_xFe_{1-x}Cr_2O_4$ , where  $x$  depends on the composition of the alloy; small amounts of other metals such as cobalt may also be incorporated and in the

primary coolant this gives rise to radiation fields from  $^{58}\text{Co}$  and  $^{60}\text{Co}$ . The outer-oxide layers are variants of the inverse spinel magnetite and are designated as  $\text{Ni}_x\text{Fe}_{3-x}\text{O}_4$ ; again,  $x$  depends on the composition of the underlying alloy but also, since the layer is precipitated from solution, it depends upon the metals dissolved in the coolant and originating in the rest of the circuit [Cook et al., 2000]. In PWRs, the composition of the outer layers on the alloys approximates  $\text{Ni}_{0.6}\text{Fe}_{2.4}\text{O}_4$ , a variant of nickel ferrite (or trevorite,  $\text{NiFe}_2\text{O}_4$ ). This also approximates the composition of the particulate matter (called “crud”) that circulates in suspension in the primary coolant at concentrations of the order of a ppb (part per billion) or less and that forms deposits on in-core fuel assemblies. In CANDU primary coolants the large surface area of carbon steel feeders makes magnetite the predominant constituent of crud.

The boiling water reactors (BWRs) traditionally operate under conditions of normal water chemistry, NWC, which exposes their alloys to high-temperature water that is slightly oxidising. This favours the formation of soluble Cr(VI) rather than the Cr(III), which is the basis of the chromite oxides that are widespread in the PWRs. Consequently, the stainless steels that constitute much of the BWR circuits develop oxides with less  $\text{FeCr}_2\text{O}_4$ ; they also contain the Fe(III) oxide  $\text{Fe}_2\text{O}_3$ , haematite. In the move to less-oxidising coolant chemistry in the BWRs, accomplished by adding hydrogen to the feedwater to create hydrogen water chemistry (HWC), the oxides on stainless steel approach those found in the PWRs. It is interesting to note that detailed in-situ studies of corrosion rates on type SA 316L stainless steel indicate that NWC conditions are somewhat less corrosive than HWC conditions [Ishida and Lister, 2012]. The corrosion for the first 100 – 150 h under NWC follows logarithmic kinetics whereas under HWC it follows a joint parabolic-logarithmic law.

#### 4.1.3 Corrosion and degradation of zirconium

In the water-cooled reactors, the major in-core materials in contact with the coolant are alloys of zirconium. The CANDUs have fuel bundles of the dioxide of natural uranium (i.e., 99.3%  $^{238}\text{U}$ , 0.7%  $^{235}\text{U}$  as  $\text{UO}_2$ ) sheathed in Zircaloy-4 and the bundles are contained in pressure-tubes of Zr-2.5%Nb. Typical fuel burnups in CANDUs are about 7 MWd/kg and on-power refuelling is necessary to maintain the core critical. The PWRs traditionally use Zircaloy-4 to clad their fuel assemblies containing enriched  $\text{UO}_2$ ; however, with the higher enrichment of 3-4%  $^{235}\text{U}$  in advanced fuel, which can achieve burnups up to 52 MWd/kg, alloys containing Nb that are more corrosion- and hydriding-resistant, such as Zirlo<sup>®</sup>, tend to be employed. The BWR fuel assemblies can reach somewhat lower burnups of up to 42 MWd/kg and have their fuel clad with Zircaloy-2. Both types of LWR (light water reactor – PWR or BWR) have batch refuelling.

The corrosion of zirconium alloys has been postulated as occurring in three stages, as shown in Figure 5. The stages have been characterized as [Hillner et al., 2000]:

- Pre-transition, when a thin, black, tightly-adherent oxide thickens according to sub-parabolic (often assumed cubic) kinetics.
- Transitory, apparently corresponding to successive “cubic” periods of decreasing duration, when the thickening film cracks and becomes porous and new oxide grows at the M-O.

- Post-transition, when kinetics become rapid and linear and white or grey oxide is formed.

As indicated in Figure 7, the transitory period was not recognized in early models, although the omission has little effect on the general description. The transition occurs at film thicknesses of 2–5  $\mu\text{m}$ .

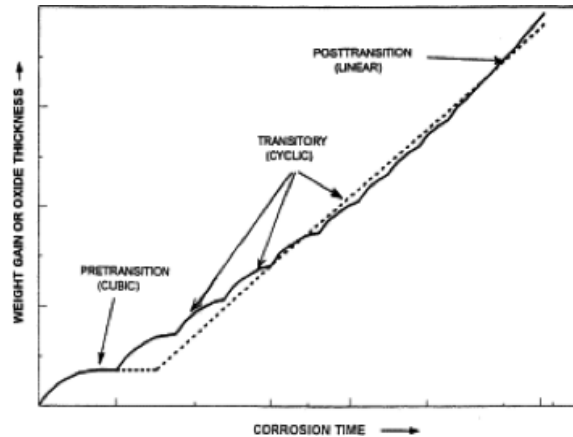


**Figure 7. Schematic diagram of Zircaloy corrosion in high-temperature water, showing three regions (dotted line indicates early assumed pre-transition cubic and post-transition linear kinetics) [Hillner et al, 2000]**

Much of the early research leading to our understanding of the corrosion and hydriding of zirconium and its alloys was conducted by Cox [Cox, 1976]. The basic electrochemical reaction is the formation of a compact oxide film based on zirconia ( $\text{ZrO}_2$ ) via:



The pre-transition film is adherent and compact zirconia of tetragonal crystal structure that grows via the solid-state diffusion through the oxide of ions/vacancies and electrons/holes. Electron diffusion is rate-determining and drives the cathodic reaction by reducing water to form hydrogen. The hydrogen generated (in overall terms by (20)) enters the metal in atomic form and at high enough concentrations precipitates within the lattice as flakes of hydride of nominal composition between  $\text{ZrH}$  and  $\text{ZrH}_2$ , making the material brittle. The post-transition oxide has monoclinic crystal structure and is much less protective than the pre-transition oxide, hence the accelerated corrosion. Since these processes occur with no oxide dissolution or release of cations to the coolant, the weight-gain of laboratory specimens is an accurate gauge of corrosion.

The oxide thicknesses on Zircaloy-4 cladding on high-burnup PWR fuel may reach 100  $\mu\text{m}$  or more but on the advanced alloys are generally less than half that amount. Concentrations of  $\text{LiOH}$  of more than  $\sim 4$  ppm (parts per million) may exacerbate corrosion rate. BWR exposures of Zircaloy-2-clad fuel induce nodular corrosion, whereby white spots of thick oxide appear on the underlying black oxide and grow with increasing exposure. The severity of nodular corrosion

depends upon the metallurgy of the alloy and the aggressiveness of the environment, but rarely causes problems (although spalled oxide has occasionally caused abrasion damage in BWR control-rod drive mechanisms). So-called “shadow corrosion”, where galvanic effects thicken  $ZrO_2$  films in proximity to components made of non-zirconium alloys such as stainless steel control-blade handles, is an additional mechanism in the low-conductivity and low-hydrogen environment of the BWR. BWR fuel is also subject to increased corrosion when the surface temperature is increased by the deposition of copper-containing crud that impairs the nucleation of steam bubbles. Such “CILC” (crud-induced localized corrosion) has led to fuel failures. These mechanisms of corrosion of zirconium alloys are reviewed in detail in the report of Adamson et al. [2007].

Because of its relatively low burn-up, CANDU fuel sheathing develops a very thin, protective oxide and failures from coolant-induced general corrosion are almost non-existent. The Zr-2.5%Nb pressure tubes in CANDUs and other PHWRs also experience low corrosion rates and their general corrosion over the 20-30-year lifetime in-reactor is acceptable. The oxidation, however, does force hydrogen (actually, deuterium from the heavy-water coolant) into the metal lattice, and this is much aggravated by deuterium that migrates into the pressure-tube ends across the rolled-joint between it and the stainless-steel end fittings, which also experience general corrosion. Hydriding (deuteriding) can then be a problem if concentrations exceed the “terminal solid solubility” (TSS), leading to precipitation of hydride “platelets”, brittleness and possible cracking if excessive stresses are experienced [Simpson et al., 1974]. In fact as mentioned earlier, in the past, pressure tubes have failed because of delayed hydride cracking (DHC), so they must be continually monitored for uptake of hydrogen/deuterium during service [Perryman, 1978].

The Zr-Nb alloy of CANDU pressure tubes is subject to several other forms of degradation (growth and creep), and these will be life-limiting for the components in one form or another and are the primary reason a mid-life refurbishment (after approximately 30 years of operation) is required on CANDU reactors. As described in Section 2.1 above, neutron irradiation causes an increase in strength and a loss of ductility (or loss of toughness) in Zr-2.5%Nb alloys (as it does in all metals) but this does not prevent the pressure tubes from performing their role as a pressure boundary. The neutron irradiation causes additional defects (dislocations) to be produced in the metal lattice, which move through the metal’s crystal structure either under the action of stress (known as radiation induced creep) or by the action of the neutron flux alone (radiation induced growth). The migration of the dislocations results in extension or contraction of the tube in its three major directions but because of the tube’s texture or predominant grain orientation, growth is concentrated in the longitudinal direction. Providing sliding bearings on each end fitting has been demonstrated to accommodate the radiation induced growth and elongation. In early CANDU designs, channel extension was only sufficient to allow for thermal and pressure-based expansion. Design changes have substantially increased the channel extension capability. Fixing one end of the fuel channel now accommodates full-life channel elongation allowing for extension to occur at the opposite, free end of the channel. Typically, at the midway point through the reactor core’s operating lifetime, the fuel channel is released at the initially fixed end and then pushed to its maximum inboard position and fixed at the formerly free end, allowing for the full scope of the design extension to be used. Fuel channel elongation is great-

est in the high power channels in the centre of the reactor resulting in a dish-shaped profile of fuel channel extension. Differential elongation could cause feeder pipes at reactor ends to contact and chafe each other, which must be avoided. Because of the material condition of the Zr-2 calandria tubes, they do not elongate to the extent of applying significant loads on the end shields.

The pressure tubes also sag with increased exposure time due to the elongation described above and from diametral creep. The diametral creep meant that fuel channels in the middle of the core, where the combination of neutron flux, pressure and temperature are highest, would suffer from significant portions of the coolant flow by-passing the fuel bundles, reducing the heat transfer efficiency and leading to reductions in the margins to dry-out. The remedy was then to derate – reduce the reactor power. Pressure-tube/calandria-tube sag also meant that the pressure tubes in some reactors approached the calandria tubes closely, and occasionally may have contacted one of the horizontal reactivity mechanism control tubes spanning the calandria. The pressure tube and its matching calandria tube are separated by wire wound toroidal spacers or garter springs that accommodate relative movement between the two. The pressure tube will sag more between the spacers than will the calandria tube due to the higher temperature and pressure operation and the weight of the fuel bundles. Should the spacers move out of position from vibration during operation, there is a risk that the hot pressure tube touches the cool calandria tube inducing a thermal gradient or “cold spot” on the wall of the pressure tube. This will cause any hydrogen/deuterium in the vicinity to diffuse down the temperature gradient and form a hydride or hydrogen blister at the surface. Above a certain size, the blister will crack to accommodate the volume change and may initiate a delayed hydride crack that could penetrate the tube wall. As these degradation problems worsened with time of operation, pressure-tube rehabilitation programs were undertaken. REFAB (Repositioning End Fitting And Bearing) involved shifting pressure tubes within the core so that they were at the start of their travel on the bearings to accommodate elongation, as described above. SLAR (Spacer Location and Repositioning) involved using electromagnetic induction to find the spacers separating the pressure tubes and calandria tubes and then shift them to their design positions to counteract sag and avoid subsequent contact. Severely affected fuel channels could have their tubes replaced, and in the extreme case LSFCR (Large Scale Fuel Channel Replacement) could be undertaken, in which a full core is replaced. This was done during the early operation at Pickering, when the pressure tubes suffered delayed hydride cracking (DHC) because of faulty installation; it is an integral part of reactor refurbishment to double the operating life of the CANDU plant.

## 4.2 Flow-Accelerated Corrosion (FAC)

Flow-accelerated corrosion (FAC), sometimes called flow-assisted corrosion, was formerly referred to as erosion-corrosion, but the last term is now usually confined to attack in a corrosive medium aggravated by mechanical forces such as those arising from abrasion by solid particles. FAC is a form of general corrosion, but it is classified on its own here because of its particularly aggressive nature. Attacking the carbon steel piping of feedwater systems, it is one of the most widespread causes of shutdown in all kinds of steam-raising plant and on occasions has led to pipe rupture with accompanying injuries and even deaths of plant personnel. Fatal

accidents due to FAC in condensate systems have occurred in at least two nuclear plants – the Surry PWR in the US in 1986 and the Mihama 3 PWR in Japan in 2004 – and at fossil-fired plants such as the Pleasant Prairie coal-fired station in the US in 1995. Unexpected and sometimes excessive pipe-wall thinning from FAC has also been an endemic problem in the outlet feeders in the primary coolant systems of the CANDU reactors that were in operation before the two CANDU 6 models in Qinshan, China, that went into service in 2002 and 2003. Some feeders have had to be replaced as they reached their minimum wall thickness long before their design lifetime. Although these replaced feeders represent a small fraction of the total number in service, the necessity of regular inspections to ensure suitable margins still remains for the pipe wall thickness; feeder FAC represents a considerable cost to plant operators through planning, conducting and verifying the field inspections in the restricted, high radiation dose area.

The basic mechanism of FAC in power plants is the dissolution and “wearing” of the normally-protective film of magnetite that develops on the corroding steel in high-temperature water. As its title suggests, the phenomenon is exacerbated by fluid flow – specifically, turbulence. As it proceeds, the attack “sculpts” the metal surface into a characteristic pattern of shallow hollows, called scallops, the size of which is governed by the turbulence (see Figure 8). The magnetite dissolves at its interface with the coolant (i.e., at the O-C, by the reverse of Equation 17) and is replenished by corrosion at the metal-oxide interface (M-O) by reactions described above for general corrosion (in overall terms by Equation 7). Also as described above, not all the corroded iron can be accommodated as oxide at the M-O – about half diffuses through the oxide to the O-C. In an FAC environment the coolant is depleted of dissolved iron, no outer layer of magnetite can precipitate and the diffused iron is transported to the bulk coolant along with that produced by the magnetite dissolution. The transport to the bulk is effected by mass transfer, which is governed by the convective processes in the coolant – i.e., by the turbulence. Since the diffusion of iron through the oxide film governs the corrosion rate, the thickness of the film attains a steady-state which then controls the FAC at a constant rate.

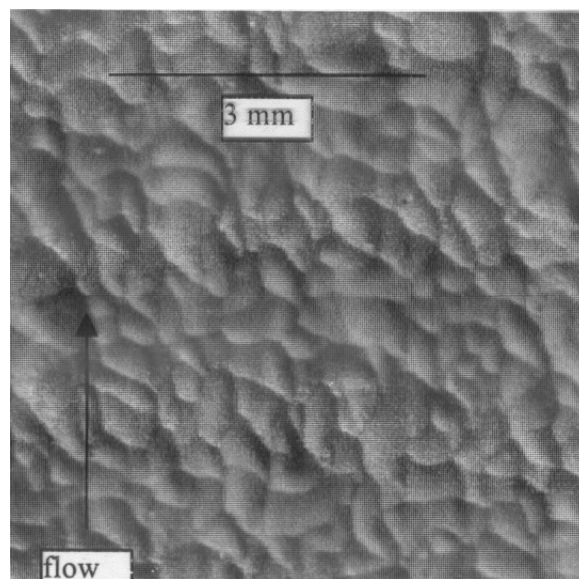


**Figure 8. Scalloped surface of outlet feeder from Point Lepreau CANDU**

This simple view of FAC, in which there are two processes in series – the dissolution of the magnetite film and the transport of iron to the bulk coolant – has been described by Equation 21 [Berge et al., 1980]:

$$R = \frac{k_m k_d (C_s - C_b)}{0.5k_m + k_d} \quad (21)$$

where:  $R$  is the FAC rate ( $\text{gFe}/\text{cm}^2 \cdot \text{s}$ ),  $k_m$  is the mass transfer coefficient ( $\text{cm}/\text{s}$ ),  $k_d$  is the magnetite dissolution rate constant ( $\text{cm}/\text{s}$ ),  $C_s$  is the magnetite solubility ( $\text{gFe}/\text{cm}^3$ ) and  $C_b$  is the concentration of iron in the bulk coolant ( $\text{gFe}/\text{cm}^3$ ). High alkalinity reduces FAC in feedwater systems by reducing magnetite dissolution (by reducing  $C_s$  and  $k_d$ ) – although at the higher temperatures in primary coolant systems increasing alkalinity tends to increase magnetite dissolution and is expected to increase FAC accordingly. The effects of flow and pH in the mechanism of FAC are shown in Figure 9.

We note that if dissolution controls,  $k_d \ll k_m$  and Equation 21 reverts to:

$$R = 2k_d (C_s - C_b) \quad (22)$$

Conversely, if mass transfer controls,  $k_m \ll k_d$  and we have:

$$R = k_m (C_s - C_b) \quad (23)$$

However, mass transfer cannot be the sole mechanism responsible for FAC, since dependences on flow rate much greater than those conventionally described by empirical mass-transfer correlations are frequently encountered; moreover, FAC often occurs in circumstances where the dissolution of the magnetite is much slower than mass transfer and should control the rate, leading to the untenable situation of the process's being described by Equation 22, which has no flow dependence at all. These observations have led to the postulate of a mechanism for FAC wherein rapidly-flowing coolant that is unsaturated in dissolved iron dissolves the magnetite (as in the conventional description) but the dissolution loosens the nano-crystals of oxide at the O-C which are then stripped from the surface (eroded or spalled) by the force of the fluid shear stress at the pipe wall [Lister and Uchida, 2010]. A schematic view of the overall mechanism, which also involves some of the reactions of magnetite and hydrogen along with the diffusion of dissolved iron through the (now single-layered) oxide film as described earlier for general corrosion, is presented in Figure 10.

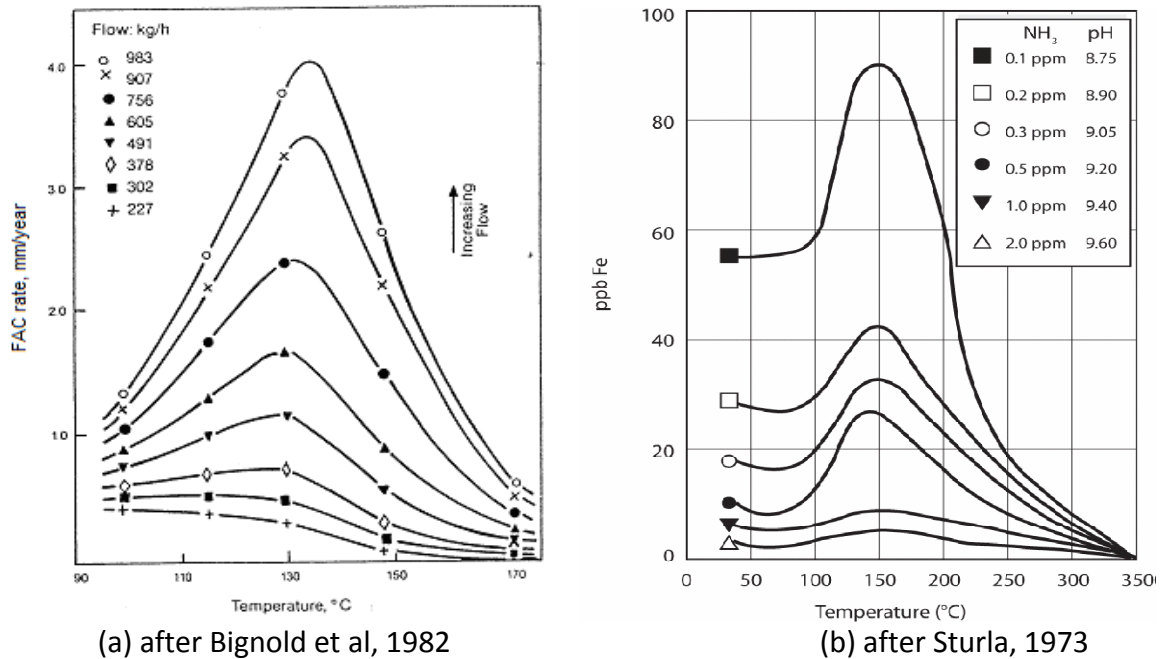


Figure 9. (a) Effect of temperature and flow on FAC at  $\text{pH}_{25^\circ\text{C}}$  9.0 with ammonia; (b) Effect of temperature and pH on the solubility of magnetite.

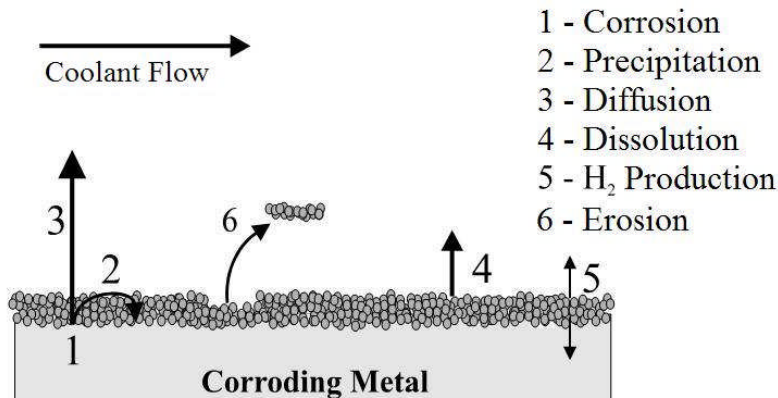


Figure 10. The overall mechanism of flow-accelerated corrosion.

The mathematical model describing this mechanism was first applied to a CANDU primary coolant system, for which measured values of  $k_d$  [Balakrishnan, 1977] were so much less than  $k_m$  that the conventional explanation of FAC via Equation 21 was clearly inadequate. The FAC in several outlet feeders at the Point Lepreau CANDU was modelled, leading to predictions of wall thinning rate around the first couple of bends downstream of the end-fitting that corresponded very well to plant measurements. At the same time, the oxide spalling terms led to realistic estimates of crud levels (concentrations of suspended oxide particles) in the primary coolant. After replacement of the dissolution terms in the model with precipitation terms and insertion of appropriate coolant flow rates and temperatures, the corrosion and oxide build-up on inlet feeders were also predicted very well, [Lister and Lang, 2002].

Traces of some transition metals (copper, molybdenum and especially chromium) in the carbon steel have long been known to reduce FAC rates; concentrations of Cr as low as a fraction of a percent have been demonstrated to lower FAC rates drastically [Bouchacourt, 1987]. Unfortunately, the existence of a lower limit of Cr content of 0.03 – 0.04%, below which FAC rates are not affected, has been propounded and is apparently incorporated into some examples of FAC software. Recent work, however, has demonstrated a reduction of ~60% in FAC rate between steels containing 0.001% Cr and those containing 0.019% Cr [Lister and Uchida, 2010].

The FAC of CANDU outlet feeders has now been mitigated in replacement piping and in new reactors by specifying a carbon steel with a higher chromium content [Tapping, 2008]. The original material had been specified with a low cobalt content to minimise the build-up of out-core radiation fields from  $^{60}\text{Co}$  during reactor operation, and this resulted in a low chromium content since no Cr concentration was specified; for example, the Point Lepreau feeders were made of A106 Grade-B steel with 0.019% Cr. Replacement material has been A106 Grade-C steel with a Cr content of ~0.33% and this has led to a reduction in FAC rate of around 50%, which should be enough to assure the integrity of the piping for the lifetime of the plant.

The lower temperatures in secondary coolants and feedwater systems lead to higher magnetite solubilities and correspondingly higher FAC rates than in primary coolants (both solubility and FAC rate peak at ~130-150°C, irrespective of pH or flow – see Figure 9). Thus, even with a steel containing 0.3% Cr and carrying feedwater dosed with amines, the 56 cm-diameter piping at the Mihama-3 PWR at 140°C corroded at an average rate of 0.3-0.4 mm/year over the 20 years or so of operation before rupturing when the wall thickness reached about 2 mm. The mechanisms of FAC in feedwater systems of Mihama and elsewhere, including the effects of steel composition, have been successfully modelled (Phromwong et al., 2011).

### 4.3 Galvanic Corrosion

The aqueous corrosion of metals involves the transfer of electrons – it is an electrochemical process. Thus, for the corrosion of iron or steel in pure water, Equation 13 represents the anodic “half-cell” process forming iron ions in solution and electrons that are conducted to adjacent sites and react with water molecules (via Equation 14 – the cathodic “half-cell” process) to form hydroxide ions and hydrogen. The anodic reaction must be balanced by the cathodic reaction. The ions in solution interact and form iron hydroxide that will precipitate as the basis for rust or, at high temperature, will form magnetite.

A metal in contact with a solution establishes an electrical potential with respect to the solution. Such a potential cannot be measured directly, since a conductor introduced into the solution to serve as a measuring electrode to indicate the potential difference with the metal will establish its own potential. The best we can do is then to measure the metal’s potential with respect to an electrode that is designated a standard. Such a standard is the “standard hydrogen electrode” (SHE), which is platinum metal in a solution of hydrogen ions at unit activity (i.e., an acid at pH 0) in contact with hydrogen gas at unit activity (i.e., at 1 atm pressure or partial pressure). The SHE is given the potential zero, and the potentials of metals in equilibrium with solutions of their own ions at unit activity are listed against the SHE potential (see Table 5). This list is the

galvanic series for industrially-important metals, and those with high potentials are termed more “noble” than those “active” ones with low potentials. An active metal can displace a more noble metal from solution – so in principle, a metal with a negative potential can displace hydrogen from solution as it dissolves or corrodes; a familiar example is the coating of an iron nail with copper as it is dipped into copper sulphate solution. Note, however, that some active metals such as aluminum and chromium are corrosion-resistant in many aqueous and atmospheric environments. This is because they form a very protective oxide that resists corrosion and makes their behavior more noble (they “passivate”).

Two dissimilar metals in contact in an aqueous environment can therefore act as an electrochemical cell, in which the more noble metal acts as the cathode and the more active metal acts as the anode; i.e., the more active metal dissolves – it corrodes. The greater the difference in the potentials, the greater the reaction rate. This is the principle of batteries such as the Daniel cell, in which electrodes of copper and zinc immersed in sulphate solution generate a potential difference of ~1.1 V as the Zn anode oxidizes and dissolves while Cu species are reduced and precipitated as metal at the Cu cathode. These processes generate an electric current in an external circuit. Galvanic coupling of metals is to be avoided in power plants, otherwise the more active metal will tend to corrode adjacent to the contact point. The severity of the corrosion depends upon the conductivity of the solution and the integrity of the joint between the metals. Oxide films may act as insulators, for example, and reduce the galvanic effect. On the other hand, galvanic processes can be used to protect metals from general corrosion. Galvanising steel by coating with zinc, for example, promotes a galvanic process, since the more active

**Table 5. The galvanic series for important metals**

Metal-metal-ion Equilibrium		Potential (25°C) Volts vs SHE
$Au^{3+} + 3e^- \rightleftharpoons Au$		+1.498
$Pt^{2+} + 2e^- \rightleftharpoons Pt$		+1.200
$Pd^{2+} + 2e^- \rightleftharpoons Pd$	↑	+0.987
$Ag^+ + e^- \rightleftharpoons Ag$	More Noble	+0.799
$Hg_2^{2+} + 2e^- \rightleftharpoons 2Hg$		+0.797
$Cu^{2+} + 2e^- \rightleftharpoons Cu$		+0.377
$2H^+ + 2e^- \rightleftharpoons H_2$		0.000
$Pb^{2+} + 2e^- \rightleftharpoons Pb$		-0.126
$Sn^{2+} + 2e^- \rightleftharpoons Sn$		-0.136
$Ni^{2+} + 2e^- \rightleftharpoons Ni$		-0.250
$Co^{2+} + 2e^- \rightleftharpoons Co$	More Active	-0.277
$Cd^{2+} + 2e^- \rightleftharpoons Cd$	↓	-0.403
$Fe^{2+} + 2e^- \rightleftharpoons Fe$		-0.440
$Cr^{3+} + 3e^- \rightleftharpoons Cr$		-0.744
$Zn^{2+} + 2e^- \rightleftharpoons Zn$		-0.763
$Al^{3+} + 3e^- \rightleftharpoons Al$		-1.662
$Mg^{2+} + 2e^- \rightleftharpoons Mg$		-2.363
$Na^+ + e^- \rightleftharpoons Na$		-2.714
$K^+ + e^- \rightleftharpoons K$		-2.925
$Li^+ + e^- \rightleftharpoons Li$		-3.040

zinc becomes the anode when the couple is immersed in a solution and lowers the potential of any areas of exposed steel, protecting them cathodically. Similarly, components prone to corrode in aqueous environments may be protected cathodically by connecting them to an electrical source or by attaching a sacrificial anode of more active metal to lower their potential.

It is important to note that in most galvanic couples it is the cathodic component that controls the reaction rate and therefore the corrosion rate. Consequently, if dissimilar metals must be in contact, the area of the cathode should be small relative to that of the anode. It follows that to protect an active metal in contact with a more noble one by coating, painting, etc., the cathode (more noble component) should be the one coated. Horror stories abound of components such as carbon steel heat exchanger shells corroding rapidly adjacent to tube sheets of more noble metals such as titanium because the steel was coated as a protective measure rather than the titanium.

In summary, measures to minimize galvanic corrosion include: selecting metals as close together as possible in the galvanic series; avoiding small-anode/large-cathode combinations (e.g.,

choosing fasteners of more noble material); insulating dissimilar metals (e.g., sleeving bolts in flanged joints, as well as using insulating washers); applying coatings carefully, and keeping them in good condition (especially those on anodes); avoiding threaded joints where possible; designing for the anodic members (making them thicker, easily replaceable, etc.); and, installing a third metal that is anodic to **both** in the couple.

#### 4.4 Stress-Corrosion Cracking & IGA

Stress-corrosion cracking (SCC) occurs in many metals in many environments; even nominally ductile materials can be affected. The attack may be trans-granular or inter-granular, depending upon whether the crack path traverses the metal grains or follows the grain boundaries (see Figure 11).

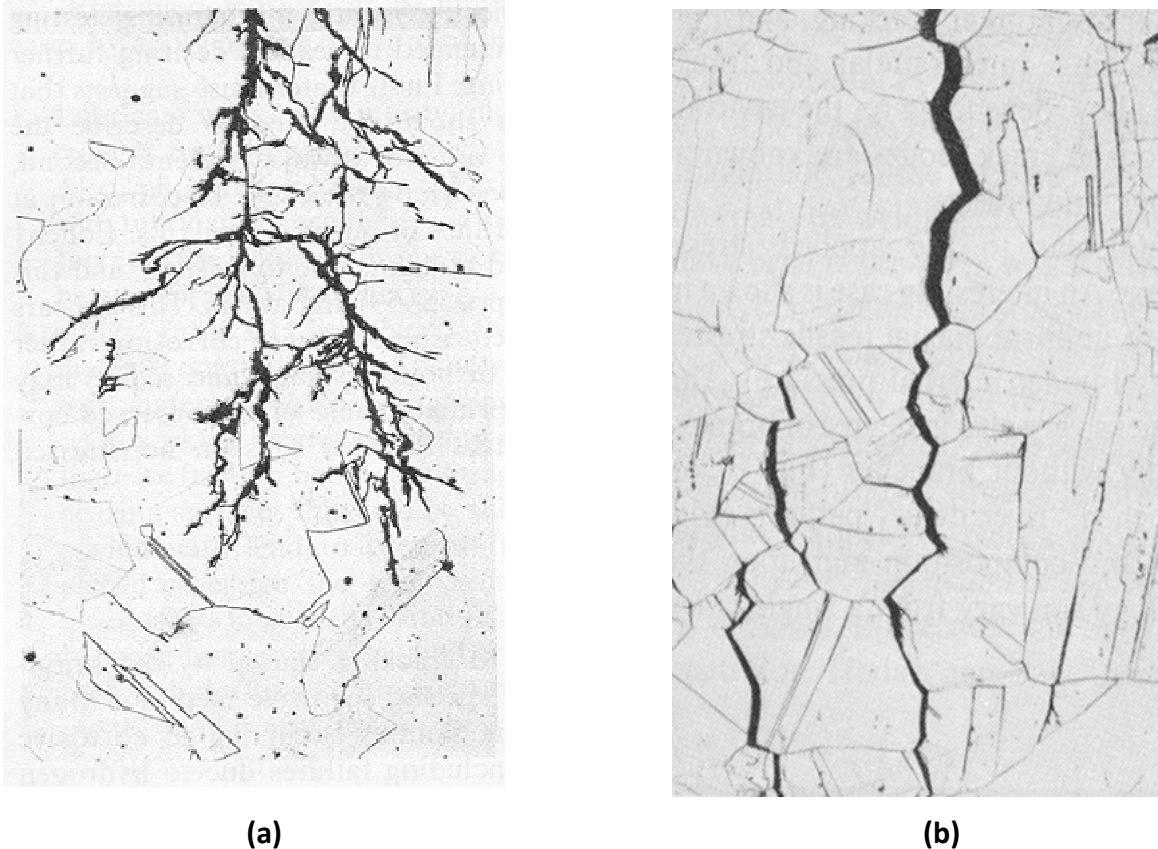


**Figure 11. Examples of transgranular (TGSCC) (a) and intergranular (IGSCC) (b) stress corrosion cracking in stainless steel and brass respectively (after Fontana 1986)**

There are three factors required for inducing SCC: the environment must be sufficiently aggressive, which involves temperature since high temperatures generally increase a material's susceptibility; the composition and microstructure must be susceptible, which includes effects such as sensitisation as discussed earlier; and, the metal must be under tensile stress, which may be residual stress from manufacturing and/or operational stress from contained pressure. Note, however, that threshold levels of these factors do not necessarily exist if there is a long enough

exposure time of the material (Andresen et al., 2000).

The inside surface of Zircaloy sheathing of nuclear fuel elements can crack during operation under the influence of mechanical strain and of fission products, particularly iodine, released during irradiation. The CANLUB process for coating the insides of CANDU fuel sheaths with a thin layer of graphitic material was designed to counteract SCC by acting as a lubricant and to some extent as a getter for iodine. It has made CANDU fuel tolerant to a range of conditions imposed by power ramping and is applicable to both  $\text{UO}_2$  and  $\text{ThO}_2$  fuels (Hastings et al., 2009).

The alloys most susceptible to cracking in nuclear coolants have been the austenitic steels such as the 300-series stainless steels used for LWR piping and component cladding and the austenitic nickel alloys such as Alloy 600 (Inconel-600) used for steam generator tubing and pressure vessel penetrations. Thus, in the first years of operation of BWRs, the coolant in the reactor recirculating system was treated with “normal water chemistry” – NWC, which was nominally pure water that became oxidizing with  $\sim 200$  ppb dissolved oxygen because of radiolysis in the core. The recirculation piping (made of type ASA 304 stainless steel) was then found to be prone to IGSCC. Extensive pipe replacements were necessary using, where possible, stress-relieved material containing low amounts of carbon to minimize the presence of sensitized material in service, especially in components where cold work and/or welding were used in fabrication. Lately, to make the coolant less oxidizing and therefore less aggressive to the austenitic steels around the core circuit, the chemistry has been changed to “hydrogen water chemistry” – HWC, which involves injecting hydrogen into the feedwater to counteract the radiolysis in the core. A level of  $\sim 2.0$  ppm has been used to reduce the electrochemical corrosion potential (ECP) of the steel from the region of  $+100$  to  $+300$  mV with respect to the standard hydrogen electrode (SHE), attained under NWC conditions, to  $-230$  mV (SHE) or lower – the measured threshold for SCC of stainless steel under BWR conditions. To achieve such low ECPs on all susceptible components in the reactor vessel without raising the hydrogen additions to unacceptable levels, General Electric’s NobleChem™ treatment has been applied, involving the addition of noble metal salts to the coolant to create a catalytic environment on surfaces (Hettiarachchi, 2005). Note that in CANDU reactors, the main use for the austenitic stainless steels is in the moderator system (the calandria vessel and the piping) and, at the low temperature of the circulating heavy water ( $<60^\circ\text{C}$ ), there have been no incidences of SCC since it was recognized early in the design of the CANDU reactors that the low carbon versions (L-grade) of the austenitic stainless steels were to be specified to avoid known problems associated with sensitization, especially during welding.

Early steam generators in the PWRs and the CANDUs at Bruce A and the demonstration CANDU NPD were tubed with Alloy 600, which was known to be somewhat resistant to TGSCC (transgranular stress-corrosion cracking) from chlorides, although research had indicated that under some circumstances at high temperature it could crack in pure water (Coriou et al., 1960). Unfortunately, most of those tubes had generally received only a cursory heat-treatment during manufacture; they had been “mill-annealed” (MA) and as a result were supplied in a sensitized state that in many instances led to IGSCC during operation. Early failures occurred on the primary side in further-stressed locations such as the tight-radius U-bends and the rolled area near the tubesheet. Also, IGSCC occurred on the secondary side because of contact with high

concentrations of alkaline impurities in crevices with tube support plates and under “sludge piles” on the tube sheet. Full replacement of most of the PWR steam generators tubed with MA Alloy 600 became necessary, so that now only a few remain, the rest having been replaced with those tubed with thermally-treated (TT – to relieve stresses) Alloy 690 – a nickel alloy containing more chromium and less nickel. In CANDUs and several European PWRs, Alloy 800 has been preferred for SG tubing. The Alloy 600 SGs in Units 1 & 2 at Bruce A have been replaced with those tubed with Alloy 800 following the refurbishment projects. This contains more chromium and iron than Alloy 600 and, having less than 50% nickel, is not strictly speaking a nickel alloy, although it is usually classified as such for comparison with the others. It has been relatively resistant to SCC.

Stainless steels and austenitic alloys containing moderate to high concentrations of carbon (i.e., >0.03%) are vulnerable to corrosion of their grain boundaries if they have undergone a heating process such as welding that raises the temperature to the region of 500-800°C. Heating to this range “sensitises” the material by preferentially precipitating the chromium in the grain boundaries as chromium carbide ( $\text{Cr}_{23}\text{C}_6$ ), thereby leaving the metal surface above the grain boundaries depleted in chromium that would otherwise form the passivating oxide based on  $\text{Cr}_2\text{O}_3$ . As shown in Figure 12, the grain boundaries are then subject to corrosion via intergranular attack (IGA).

In particularly aggressive environments, IGA can be severe enough to loosen metal grains which then fall out, leaving a roughened and even more vulnerable surface exposed. In welded material, the attack is often called weld decay.

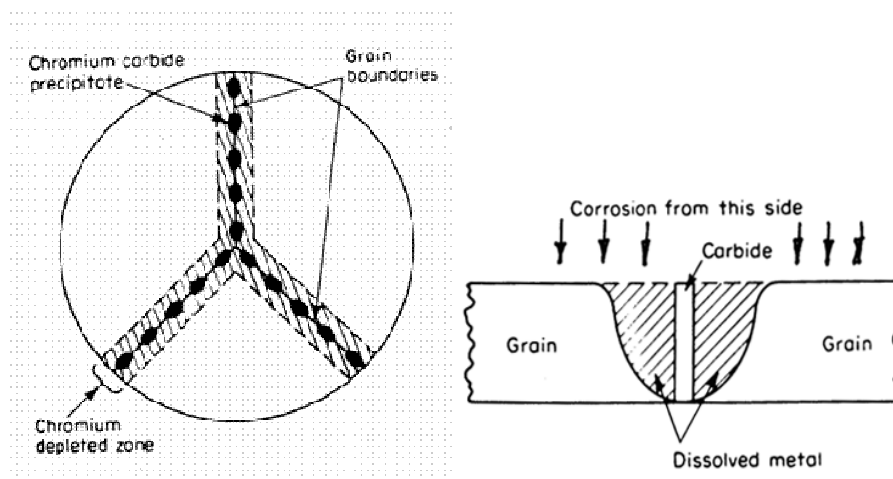


**Figure 12. Typical sensitization mode and IGA of Type 304 stainless steel (after Fontana 1986)**

Note that some situations may tolerate sensitised material; thus, sensitised stainless steel may be used in non-aggressive environments such as those found in architectural applications. For exposures to potentially aggressive conditions, however, sensitised material should not be used. A low-carbon grade of material (e.g., type ASA 304L stainless steel, with L indicating <0.03% C) is normally specified and since the carbon content is much reduced there is little available to precipitate as the carbide.

Austenitic material in general is usually supplied in the solution-quenched (also called solution-annealed or quench-annealed) condition, indicating that it was heated to above the carbide-precipitation temperature to dissolve the carbides into the metal matrix and then quenched to cool rapidly through the precipitation range of temperature so that carbide has no time to precipitate. Note that subsequent welding can re-sensitise the material, in which case the component must be solution-quenched again. There are also “stabilised” alloys such as type ASA 347 or type ASA 327 stainless steels which, respectively, contain small amounts of the strong carbide formers niobium or titanium. These have been heat-treated to precipitate the carbon as the niobium or titanium carbide at a temperature above the range where the chromium carbide would precipitate, leaving no carbon to combine with the chromium.

#### 4.5 Crevice Corrosion & Pitting

Crevice corrosion and pitting are similar in that each proceeds via an electrochemical mechanism involving the formation of differential concentration cells arising from the occlusion of chemical species within restricted areas. Beneath gaskets in flanged connections, under bolt heads and washers, within riveted and lapped joints and under deposits of sludge or silt are common areas for attack, which can occur in a wide range of environments, including cooling waters, and which is greatly exacerbated by the presence of chloride ions. As with other types of localized corrosion, metals that rely on a passivating oxide for corrosion protection, such as titanium, stainless steel, etc., are especially vulnerable, although active metals such as carbon steel are also affected. In fact, all metals are said to undergo crevice corrosion given the right conditions. The mechanism proceeds as ingress of a corroding solution into a crevice such as a lapped joint in steel, for example, initially causes metal ions (in this example  $\text{Fe}^{2+}$ ) to be released into the restricted space by the straightforward corrosion reaction. If oxygen is present in the solution it is rapidly depleted in the enclosed space and a differential aeration cell between the interior and exterior is established, promoting internal anodic metal dissolution and cathodic reduction of oxygen on surfaces external to the crevice. Even without oxygen present, the accumulated  $\text{Fe}^{2+}$  ions hydrolyse to  $\text{Fe}(\text{OH})_2$  and create internal acidic conditions while  $\text{Cl}^-$  ions are drawn into the space to maintain charge neutrality. Any oxide films within the space are degraded, the anodic processes are accelerated and attack is perpetuated (Figure 13 is a generalized illustration of the development of crevice corrosion in an aqueous environment contaminated with NaCl).

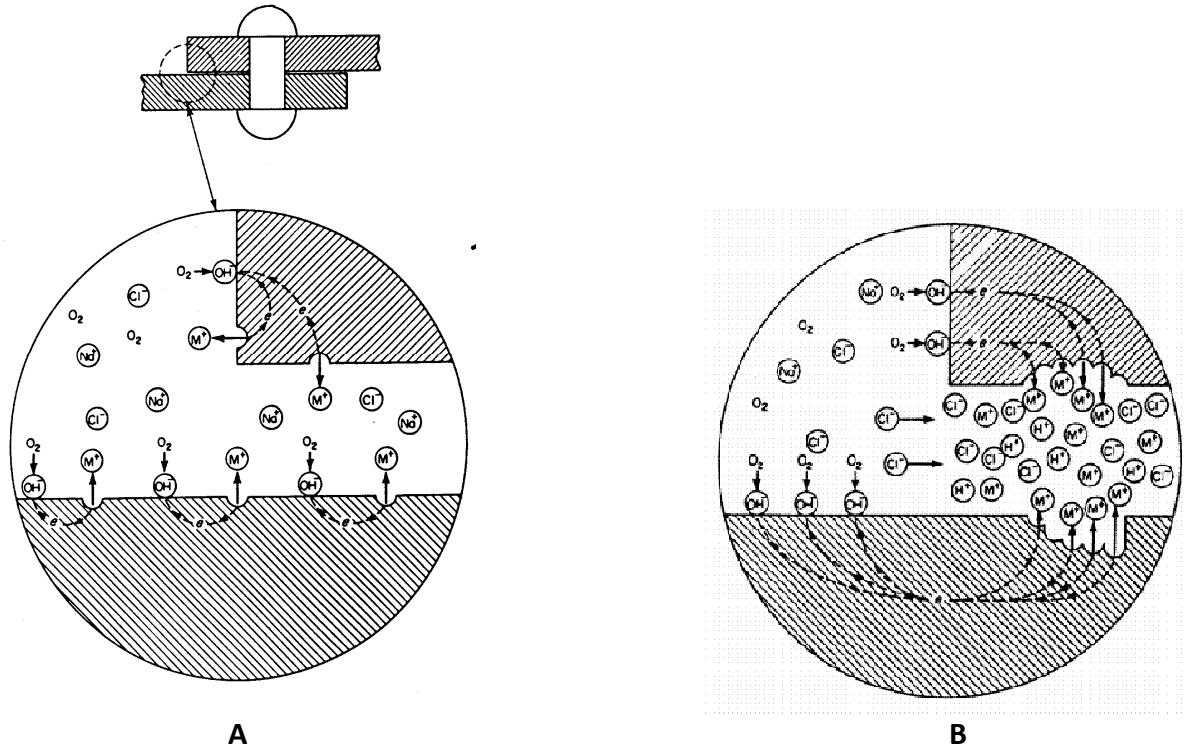


**Figure 13. Initial (A) and final (B) stages in the development of crevice corrosion of a metal M (Fontana, 1986)**

In the 1980s, the basic mechanism of the denting of the steam generators of Westinghouse design, which had drilled-hole support plates of carbon steel, was the corrosion of the steel forming the continuous crevices around the tubes. The heat transfer and boiling within the crevices drew in impurities such as chlorides and when these concentrated, especially in the presence of oxygen, aggressive acid conditions attacked the steel. The resulting growth of corrosion-product magnetite in the crevices exerted enough force to compress (“dent”) the tubes and deform the plate itself. Several steam generators have had to be replaced because of denting. The prime example in CANDUs is the crevice corrosion of the inner surfaces of pressure tubes beneath fuel bearing pads, exacerbated by localized boiling which concentrates solutes such as LiOH and leads to aggressive conditions.

The similarity of the mechanism of pitting with that of crevice corrosion can be seen in the illustration in Figure 14. Note that the precipitation of corrosion products (e.g., hydroxides in the illustrations) can occur at the mouth of the crevice and around the rim of the pit and in the latter example can grow into tubes or tubercules. Pits usually occur on upward-facing surfaces, less frequently on vertical surfaces and rarely on downward-facing surfaces, indicating an effect of gravity on the occluded high-density solution.

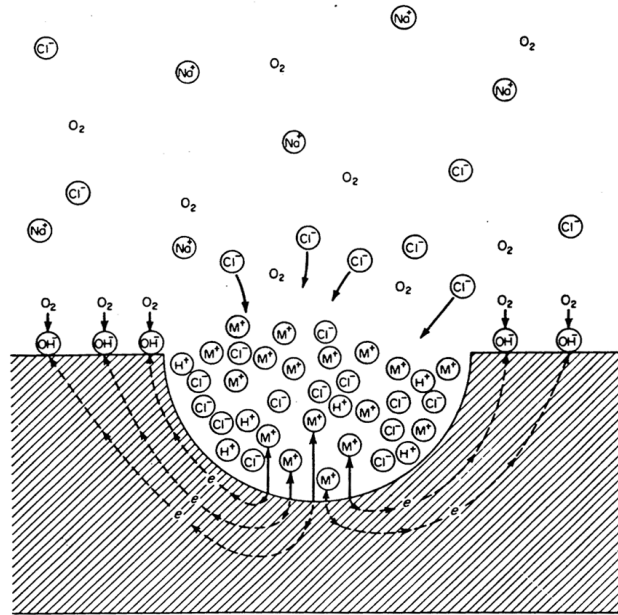


**Figure 14. Self-perpetuating corrosion pit (after Fontana, 1986)**

Pitting in particular can be extremely damaging. The pit mouths are often quite small and may be accompanied by extensive undercutting, culminating in perforation in severe cases, and pits may run into each other to create a rough surface degradation called general wastage (Figure 15). Beneath deposits, pits can go undetected and escape cursory inspections.

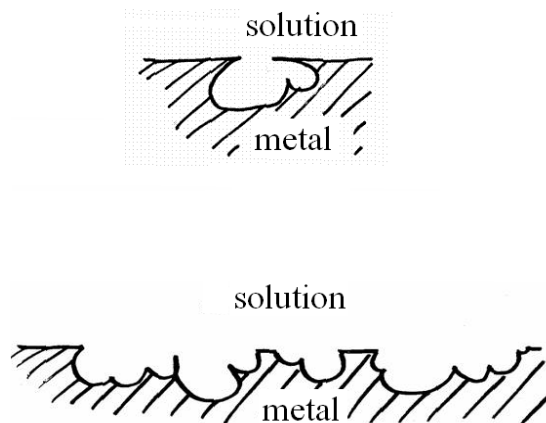


**Figure 15. An undercut pit and surface wastage from overlapping pits**

The pitting of heat exchanger tubes under silt deposits in an environment of static aerated cooling water polluted with chlorides is a pervasive problem in most industries, including nuclear power generation. Another common example in reactor systems is the pitting of the secondary side of steam generator tubes beneath sludge piles on the tubesheet. This was a particular problem with the German PWRs that had steam generators tubed with Alloy-800 and operated with chemistry controlled with additions of sodium phosphate; the concentration of aggressive species beneath the sludge led to pitting, in some cases extending to wastage. The

steam generators at the CANDU 6 at Point Lepreau, also tubed with Alloy 800, plugged many tubes because of pitting during the period of dosing with phosphate. The change from phosphate to all-volatile treatment seems to have arrested the degradation.

#### 4.6 Fretting Wear & Flow-Induced Vibration

The rubbing of one material against another can damage surfaces; in a corrosive environment the damage is exacerbated. The vibration of foreign objects trapped within components such as heat-exchanger tube bundles (known examples are condensers and steam generators) can cause rapid deterioration of the tubes and loose objects within steam generator channel heads have been known to damage tube sheets. In CANDUs and PWRs the severe conditions of flow of steam-water mixtures in the secondary side of steam generators can create excessive vibrations that cause fretting between the tubes and the tube supports. The U-bend sections of the tube bundles, where the steam quality and coolant velocities are high, are particularly susceptible. Experiments to characterise the fretting behavior of material combinations at various steam generator conditions (temperature, coolant chemistry, etc.) typically record the rate of surface damage, in terms of amount of material removed per unit time, as a function of the work rate, which is the energy dissipated by sliding contact between two surfaces per unit time. The ratio of the two, wear rate  $V$  to work rate  $W$ , defines the wear coefficient,  $K$ :

$$K = \frac{V}{W} \quad (24)$$

$K$  is usually quoted in units of  $\text{m}^2/\text{N}$ , or  $\text{Pa}^{-1}$ .

AECL at Chalk River performed an extensive series of fretting-wear tests on steam generator tube samples in contact with tube support samples. The factor having the greatest effect on tube damage was temperature;  $K$  at a steam generator operating temperature of  $265^\circ\text{C}$  was 20 times higher than at  $25^\circ\text{C}$ . Other factors, namely chemistry (ammonia, hydrazine, phosphate or boric acid), type of tube support (flat bar or broached hole), tube material (Alloy 800 or Alloy 690) or support material (type 410 or type 321 stainless steel) had relatively little effect. These results led to the suggestion that an average value of  $K$  of  $20 \times 10^{-15} \text{ Pa}^{-1}$  and a conservative value of  $40 \times 10^{-15} \text{ Pa}^{-1}$  may be used over a range of work rates for typical steam generator geometries and operating conditions (Guérout and Fisher, 1999).

Fretting wear also affects in-core components. In PWRs, it has been estimated that over 70% of fuel leaks are caused by fretting between the Zircaloy fuel rods and support grids – the so-called GRTF, grid-to-rod fretting (EPRI, 2008). The failures usually occur on final-cycle fuel assemblies, which are located at the core periphery. Similar failures occur in the WWER reactors, which have stainless steel grids.

The localized accelerated corrosion of CANDU pressure tubes because of the crevice effect beneath fuel bundle bearing pads has already been mentioned. When there is relative motion between the bearing pad and the pressure tube, resulting from flow-induced vibration for example, fretting can exacerbate the damage. This has rarely been seen except in reactors

having 13 fuel bundles, when significant damage is usually at the end of the pressure tube, where the cross-component of the coolant flow may cause more vigorous vibration. On the other hand, debris caught beneath fuel bearing pads can lead to significant fretting wear anywhere along the pressure tube and objects caught between elements within the fuel bundle can lead to fuel failures.

#### **4.7 Hydrogen Effects**

The most common form of hydrogen damage in reactor systems is the degradation of hydride-forming materials, in particular the zirconium alloys. In reactors in general these make up the fuel cladding, but in CANDUs they also make up the pressure tubes and the calandria tubes. As described earlier, delayed hydride cracking (DHC) and hydride blistering have been responsible for major replacements of CANDU pressure tubes in the past. Titanium also can be degraded by hydrogen, so it should be borne in mind that the contact of titanium components (condenser tubes, tube-sheet cladding, etc.) with carbon steel components (condenser shell, tube supports, etc.), which may promote galvanic corrosion of the steel, will drive cathodically-generated hydrogen into the metal. Similarly, hydriding of titanium condenser tubing in contact with an aluminum-bronze tube sheet occurred at the CANDU 6 at Point Lepreau. The condenser was completely re-tubed during the refurbishment outage and the Al-bronze tube sheet replaced with titanium. It follows that cathodic-protection measures such as sacrificial anodes, which lead to the production of hydrogen on cathodic components, can also promote hydriding of susceptible metals.

#### **4.8 Microbiologically-Induced Corrosion (MIC)**

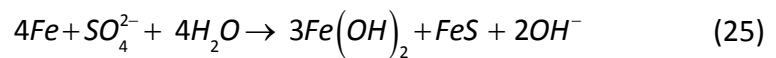
Although MIC has been known for over 70 years, it has only been recognized as a serious corrosion mechanism in nuclear and fossil plants for 30 or so years (EPRI, 1988). Early references to the subject were general descriptions of practical situations (Uhlig, 1948) and mechanistic interpretations of observations were attempted from the 1960s onwards (Videla and Herrera, 2005).

There are many types of microbe that influence corrosion and they occur in many environments, especially natural waters. Consuming a variety of nutrients, they can grow under a wide range of temperatures, pressures and alkalinities/acidities. Their spores are even more resistant to adverse conditions and can be transported around systems and lie dormant for years before being revived to germinate, attach to surfaces and create localized colonies that exude corrosive waste matter (Licina and Cubicciotti, 1989). The biofilms created by the colonies consist of the so-called exopolymers, largely consisting of polysaccharides that develop as slimes containing corrosion products and debris carried from elsewhere in the system. They impede the transport of corrosion inhibitors to the metal surface and to some extent they shield the organisms from attack by treatment chemicals such as biocides. They can be tenacious and difficult to remove by fluid forces alone and in some cases – often carbon steel piping systems – can be thick enough to cause severe pressure drops.

The microbial species may exist in anaerobic (e.g., deaerated) conditions or in aerobic (e.g.,

aerated) conditions, and in some situations the one type creates local environments that sustain the other type, giving cycles of corrosion activity. Stagnant or low-flow conditions are conducive to MIC, so components buried in damp or wet soil and water-containing piping such as fire dousing systems are particularly vulnerable. Locally stagnant environments, such as under dirt or deposits and in crevices, also promote MIC. Reactor design features with redundant, static water systems along with long shut-down periods make nuclear plants particularly susceptible. Many materials are attacked, including the common metals in reactor systems such as stainless steels, nickel alloys, carbon steel, copper, and copper alloys. Typical features of attack in carbon steel are corrosion products deposited as tubercles and in stainless steel and nickel alloys are small pits, often stained with rust, that can be deep enough to be through-wall and cause small leaks especially at welds.

Sulphate-reducing bacteria (SRB) are responsible for many failures in water systems. The species *desulfovibrio* and *desulfomaculum* are among the most widespread and economically important organisms causing corrosion. They are anaerobic because their metabolism involves the consumption of the sulphate ion in deaerated waters, especially under deposits, although they can survive limited exposures to aerated conditions. They operate in steel systems by promoting the overall mechanism:



in which the microbes are instrumental in reducing the  $\text{SO}_4^{2-}$  to  $\text{S}^{2-}$ . The early postulate that the microbes act by depolarizing the cathodic areas and catalyzing the recombination of adsorbed hydrogen atoms to molecular  $\text{H}_2$  has been largely superseded by mechanisms involving the formation of  $\text{H}_2\text{S}$  and the interaction with iron sulphide corrosion products (Videla and Herrera, 2005).

Aerobic species act by creating differential aeration and concentration cells through their biofilms. In seawater-cooled systems, for example, species such as *Pseudomonas* proliferate and can cause extensive damage to carbon steel and stainless steels. Detailed examinations of type 304 stainless steel surfaces pitted by *Pseudomonas* in seawater have shown more localized depletion of chromium in the passive films than similar control surfaces exposed in the absence of the bacteria (Yuan and Pehkonen, 2007).

Counteracting MIC is difficult. System cleanliness is quoted as a desired remedy but it should be noted that deionised water systems are susceptible. Moreover, removing slimes and biofilms by flushing is seldom effective, even with pulsating flows, and mechanical scouring with sponge balls etc. can damage protective films. Biocides are therefore a preferred recourse in many situations. Videla and Herrera (2005) list common biocides in industrial applications:

**Table 6. Biocides used in industrial water systems.**

Biocide	Properties	Usual concentration (mg/L)
Chlorine	Effective against bacteria and algae; oxidizing; pH dependent	0.1–0.2 (continuous)
Chlorine dioxide	Effective against bacteria, less so against fungi and algae; oxidizing; pH-independent	0.1–1.0
Bromine	Effective against bacteria and algae; oxidizing; wide pH range	0.05–0.1
Ozone	Effective against bacteria and biofilms; oxidizing; pH-dependent	0.2–0.5
Isothiazolones	Effective against bacteria, algae and biofilms; non-oxidizing; pH-independent	0.9–10
QUATs <sup>a</sup>	Effective against bacteria and algae; non-oxidizing; surface activity	8–35
Glutaraldehyde	Effective against bacteria, algae, fungi and biofilms; non-oxidizing; wide pH range	10–70
THPS <sup>b</sup>	Effective against bacteria, algae and fungi; low environmental toxicity; specific action against SRB	

<sup>a</sup>Quaternary ammonium compounds.

<sup>b</sup>Tetrakis-hydroxymethyl phosphonium

## 5 References

- R. Adamson, F. Garzarolli, B. Cox, A. Strasser and P. Rudling. Corrosion mechanisms in zirconium alloys. Zirart 12 Special Topic Report. A.N.T. International (2007).
- P.L. Andresen, T.M. Angeliu, R.M. Horn, W.R. Catlin and L.M. Young. Effect of deformation on SCC of unsensitized stainless steel. Proc. CORROSION 2000 Conf., Orlando, FL, USA. NACE Intern. (2000 March 26-31).
- ASM International, *ASM Handbook: Volume 9 – Metallography and Microstructures*, GF. Vander Voort, Editor, ASM, Materials Park, Ohio, 2004.
- P.V. Balakrishnan. A radiochemical technique for the study of dissolution of corrosion products in high-temperature water. *Can. J. Chem. Eng.*, 55, 357 (1977).
- P. Berge, J. Ducreux and P. Saint-Paul. Effects of chemistry on corrosion-erosion of steels in water and wet steam. Proc. 2<sup>nd</sup> Intern. Conf. on Water Chemistry of Nuclear Reactor Systems, Bournemouth, UK. BNES. (1980 October 14-17).
- G.J. Bignold, K. Garbett and I.S. Woolsey. Mechanistic Aspects of the Temperature Dependence of Erosion-Corrosion. Proc. Specialists Meeting on Erosion-Corrosion in High Temperature Water and Wet Steam. *Les Renardières, France. EDF.* (1982).

- N. Birks, G.H. Meier, F.S. Pettit, Introduction to the high-temperature oxidation of metals, 2<sup>nd</sup> Edition, Cambridge University Press, 2006.
- M. Bouchacourt. Identification of key variables: EdF studies. Proc. EPRI Workshop on Erosion-Corrosion of Carbon Steel Piping. Washington DC, USA. (1987 April).
- W.D. Callister, D.G. Rethwisch, Materials Science and Engineering: An Introduction, 8<sup>th</sup> Edition, Wiley, 2009.
- W.G. Cook, D.H. Lister and J.M. McInerney. The effects of high liquid velocity and coolant chemistry on material transport in PWR coolants. Proc. 8<sup>th</sup> Intern. Conf. on Water Chemistry of Nuclear Reactor Systems, Bournemouth, UK, BNES, October 22-26, (2000).
- H. Coriou, L. Grall, Y. Legall and S. Vettier. Stress corrosion cracking of Inconel in high temperature water. 3e Colloque Metall., Saclay, 1959. North Holland Publ., Amsterdam. p. 161 (1960).
- B. Cox. Mechanisms of zirconium alloy corrosion in nuclear reactors. J. Corr. Sci. Eng., Vol. 6, Paper 14 (2003).
- EPRI. Sourcebook for microbiologically influenced corrosion in nuclear power plants. Electric Power Research Institute. Technical Report NP-5580 (1988).
- EPRI. Fuel reliability guidelines: PWR grid-to-rod fretting. Electric Power Research Institute, Product ID 1015452. (28<sup>th</sup> July 2008).
- M.G. Fontana. Corrosion Engineering. McGraw-Hill. (1986).
- A. Garlick, R. Sumerling and G.L. Shires. Crud-induced overheating defects in water reactor fuel pins. J. Br. Nucl. Energy Soc., 16(1), 77 (1977).
- F.M. Guérout and N.J. Fisher. Steam generator fretting-wear damage: a summary of recent findings. Trans. ASME, 121, 304-310 (1999 August).
- I. Hastings, K. Bradley, J. Hopwood, P. Boczar, S. Kuran and S. Livingstone. We can use thorium. Nucl. Eng. Intern. (2009 August 28).
- S. Hettiarachchi. BWR SCC mitigation experiences with hydrogen water chemistry. Proc. 12<sup>th</sup> Intern. Conf. on Environmental Degradation of Matls. in Nuclear Power Systems. Salt Lake City, Utah, USA. TMS. (2005 August 14-18).
- E. Hillner, D.G. Franklin and J.D. Smee. Long-term corrosion of Zircaloy before and after irradiation. J. Nucl. Matls., 278(2-3), 334-45 (2000).

- K. Ishida and D.H. Lister. In-situ measurement of corrosion of Type 316 Stainless Steel in 280°C pure water via the electrical resistance of a thin wire. *J. Nucl. Sci. Tech.* 49 (11), (2012 November).
- P. Kofstad. On the formation of porosity and microchannels in growing scales. *Oxidation of Metals*, 24(5-6), 265-276 (1985).
- G.J. Licina and D. Cubicciotti. Microbial-induced corrosion in nuclear power plant materials. *J. Nucl. Matls.*, 41(12). 23-27 (1989).
- D.H. Lister. Activity transport and corrosion processes in PWRs. *Nucl. Energy*, 32(2), 103- 114 (1993).
- D.H. Lister. Some aspects of corrosion in cooling water systems and their effects on corrosion product transport. *Proc. EUROCORR 2003, Budapest, Hungary*, (2003 September 28-October 2).
- D.H. Lister and L.C Lang. A mechanistic model for predicting flow-assisted and general corrosion of carbon steel in reactor primary coolants. *Proc. Chimie 2002; Intern. Conf. Water Chem. Nucl. Reactor Systems. Avignon, France. SFEN.* (2002).
- D.H. Lister and S. Uchida. Reflections on FAC mechanisms. *Proc. Intern. Conf. on Flow-Accelerated Corrosion (FAC) in Fossil and Combined Cycle / HRSG Plants, Arlington, VA, USA.* (2010 June 29-July 1).
- E.C.W. Perryman. Pickering pressure tube cracking experience. *Nucl. Energy*, 17, 95–105 (1978).
- P. Phromwong, D.H. Lister and S. Uchida. Modelling material effects in flow accelerated corrosion. *Proc. Intern. Conf. on Environmental Degradation of Matls. in Nuclear Power Systems, Colorado Springs, CO. TMS.* (2011 August 7-11).
- E.C. Potter and G.M.W. Mann. Oxidation of mild steel in high-temperature aqueous systems. *Proc. 1<sup>st</sup> Intern. Congress Metallic Corros. London.* p. 417 (1961).
- Qiu, L. Dissolution of silicon nitride in high-temperature alkaline solutions. *Proc. Intn'l. Conf. Props. Water and Steam. IAPWS. Greenwich, London. Sept. 1<sup>st</sup>-5<sup>th</sup>* (2013).
- P.R. Roberge. *Handbook of corrosion engineering.* McGraw Hill (2000).
- G. Schikorr. On the iron-water system. *Z. Elektrochem.* 35, 62 (1928).
- C.J. Simpson and C.E. Ells. Delayed hydrogen embrittlement of Zr-2.5wt.%Nb. *J. Nucl. Mater.*, 52, 289–295 (1974).
- J.P. Slade and T.S. Gendron. Flow accelerated corrosion and cracking of carbon steel piping in

- primary water – operating experience at the Point Lepreau Generating Station. Proc. Intern. Conf. on Environmental Degradation of Matls. in Nuclear Power Systems, Salt Lake City, UT. TMS. (2005).
- P. Sturla. Oxidation and deposition phenomena in forced circulating boilers and feedwater treatment. Proc. Fifth National Feedwater Conf. Prague, Czech. (1973).
- R.L. Tapping. Materials performance in CANDU reactors: The first 30 years and the prognosis for life extension and new designs. J. Nucl. Materials. 383, 1-8 (2008).
- M.R Taylor, J.M Calvert, D.G. Lees and D.B. Meadowcroft. The mechanism of corrosion of Fe-9%Cr alloys in carbon dioxide. Oxidation of Metals, 14(6), 499-516 (1980).
- H.H Uhlig. Corrosion handbook. John Wiley, New York. 466-481 (1948).
- H.A. Videla and L.K. Herrera. Microbiologically-influenced corrosion: Looking to the future. Intern. Microbiol., 8. 169-180 (2005).
- C. Wagner and W. Traud. On the interpretation of corrosion processes through superposition of electrochemical partial processes and on the potential of mixed electrodes. Z. Elektrochem. Ang. Physik. Chemie, 44, 398 (1938).
- G.S. Was, Fundamentals of Radiation Materials Science: Metals and Alloys, Springer, 2007.
- S.J. Yuan and S.O. Pehkonen. Microbiologically influenced corrosion of 304 stainless steel by aerobic *Pseudomonas* NCIMB 2021 bacteria: AFM and XPS study. Colloids and Surfaces B: Biointerfaces, 59(1), 87-99 (2007).

## 6 Acknowledgements

The following reviewers are gratefully acknowledged for their hard work and excellent comments during the development of this Chapter. Their feedback has much improved it. Of course the responsibility for any errors or omissions lies entirely with the authors.

Kit Colman  
Mark Daymond  
Ed Price  
Bob Tapping

Thanks are also extended to Diana Bouchard for expertly editing and assembling the final copy.